The Designing of Objects using Rational Splines with Shape Control

by

Mohammed Abdul Raheem

A Thesis Presented to the

FACULTY OF THE COLLEGE OF GRADUATE STUDIES

KING FAHD UNIVERSITY OF PETROLEUM & MINERALS

DHAHRAN, SAUDI ARABIA

In Partial Fulfillment of the
Requirements for the Degree of

MASTER OF SCIENCE

In

COMPUTER SCIENCE

June, 1996

THE DESIGNING OF OBJECTS USING RATIONAL SPLINES WITH SHAPE CONTROL

BY

MOHAMMED ABDUL RAHEEM

A Thesis Presented to the

FACULTY OF THE COLLEGE OF GRADUATE STUDIES

KING FAHD UNIVERSITY OF PETROLEUM & MINERALS

DHAHRAN, SAUDI ARABIA

In Partial Fulfillment of the

Requirements for the Degree of

MASTER OF SCIENCE

In

COMPUTER SCIENCE

JUNE 1996

UMI Number: 1381997

UMI
300 North Zeeb Road
Ann Arbor, MI 48103

KING FAHD UNIVERSITY OF PETROLEUM AND MINERALS
DHAHRAN, SAUDI ARABIA

COLLEGE OF GRADUATE STUDIES

This thesis, written by **MOHAMMED ABDUL RAHEEM** under the direction of his Thesis Advisor and approved by his Thesis Committee, has been presented to and accepted by the Dean of the College of Graduate Studies, in partial fulfillment of the requirements for the degree of **MASTER OF SCIENCE** in **COMPUTER SCIENCE**.

THESIS COMMITTEE

Dr. M. Sarfraz (Thesis Advisor)

6/26/96

Dr. J. AlGhamdi (Member)

Dr. M. AlMulhem (Member)

Dr. M. AlSuwaiyel (Member)

Department Chairman

Dean, College of Graduate Studies

24-7-96

Date

ACKNOWLEDGEMENT

All praise and thanks be to Almighty Allah, the most Gracious, the most Merciful. Peace and mercy be upon His Prophet.

Acknowledgement is due to King Fahd University of Petroleum and Minerals for support of this research.

I would like to offer my indebtedness and sincere appreciation to my thesis advisor Dr. Muhammad Sarfraz, who has been a constant source of help and encouragement during this work. I also greatly appreciate the invaluable cooperation and support extended by my thesis committee members: Dr. Muhammed Al-Mulhem. Dr. Mohammad Al-Suwaiyel and Dr. Jaralla Al-Ghamdi.

I wish to express my gratitude to my parents. brother. sisters and relatives. who motivated and guided me through out my career. Finally. I thank all my friends for providing an enjoyable work atmosphere.

Contents

List of Figures

THESIS ABSTRACT

Name: MOHAMMED ABDUL RAHEEM

Title: THE DESIGNING OF OBJECTS USING RATIONAL SPLINES: WITH SHAPE CONTROL

Degree: MASTER OF SCIENCE

Major Field: INFORMATION & COMPUTER SCIENCE

Date of Degree: JUNE 1996

Interactive curve design in Computer Aided Geometric Design (CAGD) is typically accomplished through the manipulation of a control polygon. The methodology based on B-spline type basis functions results in a curve that lies in the convex hull. Changes in the control polygon only effect the curve locally. This research is oriented towards the representation of interpolatory curves and surfaces. using rational cubic splines. These interpolatory splines have been constructed through the B-spline formulation. The method for evaluating the rational cubic B-spline curve is suggested by a transformation to Bernstein-Bezier form. The method uses the cubic by quadratic functions and for given control points constructs the interpolatory spline method which enjoys all the geometric properties of B-splines. Hence the spline representation is not a spline over spline form.

The generation of interpolating spline curves and surfaces is a useful and powerful tool in CAGD. Various methods have been developed to control the shape of an interpolating curve for computer-aided design applications. Some methods are better suited for controlling the tension of the curve on an interval. while others are better suited for controlling the tension at the individual control points. This work is oriented towards investigating C^2 like rational interpolatory splines with point and interval tension. Shape controls are available to tighten the rational splines on intervals and/or at the interpolation points.

King Fahd University of Petroleum and Minerals, Dhahran.
June 1996

خلاصة الرسالة

الاسم: محمد عبد الرحيم

العنوان: تصميم الأجسام باستخدام الشرائح الجذرية: مع التحكم في الشكل

الدرجة: ماجستير في العلوم

التخصص: معلومات وعلوم الحاسب الآلي

تاريخ الدرجة: يونيو ١٩٩٦

التصميم التفاعلي للمنحنيات في مجال التصميم الهندسي بمساعدة الحاسب الآلي يتم عن طريق معالجة مضلَع التحكم. الطريقة المبنية علي شرائح ب ذات الدوال الأساسية تنتج منحنيات تقع في داخل الغلاف المحدّب. التغيرات في مضلَع التحكم يؤثر على المنحنى محليا فقط. هذا البحث يدور حول تمثيل المنحنيات والسطوح المولّدة باستخدام الشرائح الجذرية المكعبة. لقد تم بناء هذه الشرائح المولدّة عن طريق تكوين شرائح ب. تم اقتراح طريقة لتقييم منحنيات شرائح ب الجذرية المكعبة وذلك عن طريق التحويل إلي شكل برستين-بزير. الطريقة تستخدم الدوال المكعبة في الرباعية، وبالنسبة لنقاط تحكم معطاة، تبني طريقة الشرائح المولّدة التي تتمتع بكل الخواص الهندسية لشرائح ب. وبهذا، يكون تمثيل الشرائح ليس على شكل شريحة فوق شريحة.

إنتاج منحنيات وسطوح شرائح التوليد هو أداة نافعة وقوية في مجال التصميم الهندسي بمساعدة الحاسب الآلي. لقد تم تطوير عدة طرق للتحكم في شكل منحنيات التوليد بالنسبة لتطبيقات التصميم بمساعدة الحاسب الآلي. بعض الطرق أفضل من الأخرى في التحكم في شد المنحنى فوق فترة ما. البعض الآخر أفضل في التحكم في الشد عند نقاط التحكم منفردة. هذا العمل يدور حول تحقيق شرائح توليد جذرية شبيهة ب C^2 مع شد عند النقاط وفي الفترة. توجد أشكال تحكّم لربط الشرائح الجذرية في فترة و/أو عند نقطة توليد.

درجة الماجستير في العلوم

جامعة الملك فهد للبترول والمعادن

الظهران، المملكة العربية السعودية

يونيو (حزيران) ١٩٩٦م - صفر ١٤١٧هـ

Chapter 1

INTRODUCTION

Interactively designing distinct objects is a common problem of Computer Aided Design (CAD), Computer Aided Manufacturing (CAM), Solid Modelling and Graphics today. It is typically accomplished through the manipulation of a control polygon. This work is oriented towards the B-spline type approach, for the representation of curves and surfaces, using rational cubic splines. B-splines are a useful and powerful tool for CAGD and Solid Modelling, and they can be found frequently in the existing CAD/CAM systems.

Splines are used in graphics applications to design curve and surface shapes, to digitize drawings for computer storage, and to specify animation paths for the objects or the camera in a scene. Typical CAD applications for splines include the design of automobile bodies, aircraft and spacecraft surfaces, and ship hulls. In computer graphics, the term *spline curve* refers to any composite curve formed with polynomial sections satisfying specified continuity conditions at the boundary of the pieces. And a *spline surface* is described with two sets of orthogonal spline curves.

Interpolation curves are commonly used to digitize drawings or to specify animation paths, whereas approximation curves are primarily used as design tools to structure object surfaces.

Designing curves and surfaces plays an important role not only in the construction of various objects like automobiles, ship hulls, airplane fuselages and wings, propeller blades, shoe insoles, bottles, etc, but also in the description of geological, physical and even medical phenomena such as modelling the human heart etc. This thesis presents a description and analysis of the class of rational cubic splines for use in CAGD. It is proposed to use them for the representation of parametric curves and surfaces in interpolatory form. CAGD is concerned with the approximation and representation of curves and surfaces that arise when these objects have to be processed by a computer. Development of objects in computer science is mainly based on designing the curves and surfaces.

In CAD the smoothness of curves and surfaces plays an important role. Smoothness is a global as well as a local property. Various methods have been developed to control the shape of an interpolating curve such as those in [1] and [2]. Some methods are well suited for one type of shape control but not well suited for another. This research is oriented towards design of objects using rational splines. In particular given a set of data points a C^2 like rational spline which passes through the data points is investigated. The resulting rational spline is capable of controlling the shape of interpolating curves, easy to implement and computationally economical.

1.1 Notation and Conventions

1. The symbol R^N will be used to denote the N-dimensional real space.

2. Knot partitions will be assumed as

$$t_0 < t_1 < t_2 \ldots < t_m. \tag{1.1}$$

3. For any i the transformations

$$\theta \equiv \theta(t) = (t - t_i)/h_i$$

will be commonly used where

$$h_i = t_{i+1} - t_i.$$

4. Vectors (Points) and vectors valued functions are set in bold face letters.

5. F_i, $i = 0, 1, \ldots, n$ will denote the interpolatory points and Δ_i will be used for the ratios of the type

$$\Delta_i = (F_{i+1} - F_i)/h_i$$

6. D_i will be used for the first derivative value at the knot t_i.

7. Given a function such as $p(t)$, we will denote the i^{th} derivative by $p^{(i)}(t)$.

8. $p \in C^m[t_0, t_n]$ will mean that each component function of p: $[t_0, t_n] \to R^N$ is m-times continuously differentiable on $[t_0, t_n]$.

1.2 Overview

1.2.1 Definitions

1. **Spline:** An M th degree spline is a piecewise polynomial of degree M that has continuity of derivatives of order M-1 at each knot.

   In computer graphics, the term *spline curve* refers to any composite curve formed with polynomial sections satisfying specified continuity conditions at the boundary of the pieces. And a *spline surface* is described with two sets of orthogonal spline curves.

   Splines are generally classified as *interpolation* and *approximation* splines. In interpolation spline the curve passes through each control point, whereas in approximation spline, the curve generally approximates the set of control points without necessarily passing through any control point. A spline curve is described using a geometry vector of four control points, in contrast with the geometry matrix of sixteen elements used to produce a surface. Interpolation curves are commonly used to digitize drawings or to specify animation paths, whereas approximation curves are primarily used as design tools to structure object surfaces.

2. **Smoothness of curves:** Curve segments exhibit different continuity properties. When a composite curve is made up of curve segments these properties may change depending on how the segments have been joined.

(a) **Parametric continuity:** Two adjoining curves are said to posses *Zero order parametric continuity* C^0, if they simply meet *i.e* have a common join point. If the tangent vectors to each curve segment at the common join point are equal then the curve exhibits *First order parametric continuity* C^1. In general if the direction and magnitude of $d^n/dt^n[Q(u)]$ (Q(u) represents the curve) are equal at the join point between segments then the curve exhibits C^n continuity.

(b) **Geometric continuity:** Two adjoining curves are said to posses *zero order geometric continuity* (G^0) if they simply meet *i.e* have a common join point. If the tangent vectors to each curve segment at the common join point match to within a constant with directions equal, magnitudes not equal then the curve has G^1 *geometric continuity* . *Second order geometric continuity* G^2 means that both the first and second parametric derivatives of the two curve sections are proportional at their common join point.

1.2.2 Rational Splines

The rational curve has manifested itself in various forms including NURBS (non-uniform rational B-splines), the rational Bezier curve, and the rational Beta-spline. A single rational function usually does not have enough freedom to represent a given curve. Thus several rational segments are joined together to generate spline curve. Bezier (rational Bezier) and B-spline (or B-spline like) curves/surfaces are powerful tools for CAGD. They are found incorporated, in most existing CAD/CAM systems.

A rational spline is the ratio of two spline functions. General rational cubic curve segments are ratios of polynomials:

$$x(t)=X(t)/W(t), \quad y(t)=Y(t)/W(t), \quad z(t)=Z(t)/W(t)$$

Where X(t), Y(t), Z(t) and W(t) are all cubic polynomial curves whose control points are defined in homogeneous coordinates. In general, the polynomials in a rational curve can be Bezier, Hermite, or any other type. When they are B-splines, we have nonuniform rational B-splines, sometimes called NURBS [3].

Rational curves are useful for two reasons. The first and most important reason is that they are invariant under rotation, scaling, translation and perspective transformations of the control points , whereas nonrational curves are invariant under only rotation, scaling, and translation. This means that the perspective transformation needs to be applied to only the control points, which can then be used to generate the perspective transformation of the original curve. A second advantage of rational splines is that, unlike nonrationals, they can define precisely any of the conic sections. A conic can be only approximated with nonrationals, by using many control points close to the conic. This second property is useful in those applications, particularly CAD, where general curves and surfaces as well as conics are needed.

1.3 Previous Work

1.3.1 Rational Splines with Shape Control

Although the C^2 cubic splines have the many elegant mathematical properties discussed in [4] and [5], the curves sometimes exhibit undesirable oscillations. Various methods have been developed to control the shape of an interpolating curve, such as those in [1], [2], [6], and [7]. Some methods are well suited for one type of shape control but not well suited for another. For this reason, a multipurpose system was developed in [8] which consists of different spline methods and uses the particular spline that is most suited for the desired type of shape control. This system uses a C^2 cubic spline to generate the initial interpolating curve, an exponential - based spline under tension [9] and a rational spline with tension [2] are used to flatten or tighten the curve on segments between interpolation points, and piecewise cubic ν-splines [6] are used to sharpen or tighten the corners of the curve at the interpolation point. Thus, to avoid a multiplicity of methods, one method is desirable which is capable of generating a broad range of interpolating curves, is easy to implement, provides a shape control according to the user's wishes and is computationally economical.

1.3.2 Spline Interpolation

In his remarkable paper Manning [10] considered two important problems of spline interpolation:

1. How to choose the tangent vector magnitudes

2. How to compute curvature continuous cubic curve interpolants

Nu-splines were introduced by Nielson [11] as piecewise polynomial alternatives to splines under tension. Nu-splines are curvature and C^1 continuous curves that contain free parameters, the nus, used to control the arc length.

1.3.3 Interpolation using B-splines

Fitting a B-spline curve or surface through existing data points has two major applications in computer graphics. First, in modelling: a set of sample data points can be produced by a three-dimensional digitizing device, such as a laser ranger. The problem is then to fit a surface through these points so that a complete computer graphics representation is available for manipulation (for, say, animation or shape change) by a program. Second, in computer animation: we may use a parametric curve to represent the path of an object that is moving through three dimensional-space. Particular positions of the object (key frame positions) may be defined, and we require to fit a curve through these points. A B-spline curve is commonly used for this purpose because of its C^2 continuity property. In animation we are normally interested in smooth motion and a B-spline curve representing the position of an object as a function of time will guarantee this.

The problem of B-spline interpolation can be informally stated as follows: given a set of data points we require to derive a set of control points for a B-spline curve that will define a fair curve that represents the data points.

1.4 Review of some Shape Control Methods

In this section a brief review of some of the existing spline methods is given because these can be considered either as an alternative or as particular cases of the spline methods which are going to be discussed in the theory of this thesis. For each of the splines we assume the knot partition of equation(1.1) and the values $F_i, i = 0, \ldots, n$ at the knots. Throughout the discussion, we will denote the spline curve by $p(t)$

1.4.1 Cubic Spline

The natural cubic spline is the C^2 piecewise cubic function that minimizes

$$V(f) = \int_{t_0}^{t_n} (f^{(2)}(t))^2 dt \tag{1.2}$$

over all functions in $H^2[t_0, t_n]$. $H^2[t_0, t_n]$ consists of all functions whose first derivative is absolutely continuous and whose second derivative belongs to $L^2[t_0, t_n]$.

1.4.2 Spline under Tension

Barsky [9] constructs the spline under tension as the interpolating function in $H^2[t_0, t_n]$ that minimizes

$$\begin{aligned} V(f) = & \int_{t_0}^{t_n} (f^{(2)}(t))^2 dt + \\ & \sum_{i=0}^{n-1} w_i \int_{t_i}^{t_{i+1}} (f^{(1)}(t))^2 dt \end{aligned} \tag{1.3}$$

where $w_i > 0$, for $i = 0, \ldots, n-1$. The minimizing function is a piecewise exponential and linear function that belongs to C^2. The constant w_i can be used to control the tension of the curve on the interval $[t_i, t_{i+1}]$. As w_i increases, the exponential-based spline under tension becomes tighter on that interval.

1.4.3 Weighted Spline

The weighted spline in [1] is the interpolating function that minimizes

$$V(f) = \int_{t_0}^{t_n} w(t)(f^{(2)}(t))^2 dt \tag{1.4}$$

where $w(t)$ is a positive integrable function. If $w(t)$ is a piecewise constant function, then the weighted spline is a C^1 piecewise cubic polynomial. If $w(t)$ is large on one interval, relative to bordering intervals, then the weighted spline becomes tighter on that interval in a manner similar to the spline under tension. It should be noted that the spline under tension is C^2, but computationally more expensive because it is a piecewise exponential; whereas the weighted spline is a piecewise cubic, but it only belongs to C^1.

1.4.4 ν-Spline

The ν-spline in [6] is the interpolating function in $H^2[t_0, t_n]$ that minimizes

$$V(f) = \int_{t_0}^{t_n} (f^{(2)}(t))^2 dt + \sum_{i=0}^{n} \nu_i (f^{(1)}(t_i))^2 dt \tag{1.5}$$

where $\nu_i \geq 0$, for $i = 0, \ldots, n$. As noted in [6], the ν-spline is a C^1 piecewise cubic function that does not mimic splines in tension well in the functional case. However, in the parametric case, as ν_i increases the ν-spline curve becomes tighter at the i^{th} interpolation point because the magnitude of the tangent vector approaches zero.

1.4.5 Weighted ν-Spline

The weighted ν-spline [1] is the marriage of the weighted spline and the ν-spline. It is the C^1 piecewise cubic interpolatory function $p(t)$ that minimizes

$$V(f) = \sum_{i=0}^{n-1} w_i \int_{t_0}^{t_n} (f^{(2)}(t))^2 dt + \sum_{i=0}^{n} \nu_i (f^{(1)}(t_i))^2 dt \tag{1.6}$$

where $w_i > 0$ for $i = 0, \ldots, n-1$ and $\nu_i \geq 0$ for $i = 0, \ldots, n$. The ν_i are termed as point tension factors because they tighten a parametric curve at the i^{th} point in the same way as they do for the ν-splines in [6]. The w_i are termed interval weights because they tighten the curve on the i^{th} interval in the same way as they do for the weighted splines. If ν_i =0 and all $w_i = c$, where c is some constant value, then the weighted ν-spline is the C^2 cubic spline. If all $w_i = c$, then the weighted ν-spline equals the ν-spline in [6] with tension factors ν_i/c. If all ν_i=0, then it equals the weighted spline.

1.4.6 β-Spline

The β-spline [12] is a piecewise cubic function $p(t)$ that satisfies the following derivative constraints

$$\begin{bmatrix} p(t_{i+}) \\ p^{(1)}(t_{i+}) \\ p^{(2)}(t_{i+}) \end{bmatrix} = \begin{bmatrix} 1 & & \\ 0 & \beta_{1,i} & \\ 0 & \beta_{2,i} & \beta_{1,i}^2 \end{bmatrix} \begin{bmatrix} p(t_{i-}) \\ p^{(1)}(t_{i-}) \\ p^{(2)}(t_{i-}) \end{bmatrix} \tag{1.7}$$

Where $\beta_{1,i} \geq 1$, $i = 0, \ldots, n-1$ and $\beta_{2,i} \geq 0$, $i = 0, \ldots, n$. The $\beta_{1,i}$ are known as biased tension factors as they pull the curve to the one side. The parameters $\beta_{2,i}$

are known as point tension factors because they behave in exactly similar way as the ν_i in the ν-splines. If $\beta_{2,i} = 0$ and $\beta_{1,i} = 1$, then the β-spline is the C^2 cubic spline. If $\beta_{1,i} = 1$, then it equals the ν-spline. For parametric curves, the constraints of equation(1.7) mean that the curve is GC^2 (geometric continuity of order 2).

1.5 Proposed Work

1.5.1 Problem Formulation

The following interpolatory B-spline like rational splines have been investigated:

1. Interpolatory rational cubic spline with point tension
2. Interpolatory rational cubic spline with interval tension
3. Interpolatory rational cubic spline with point and interval tension.

The foremost objective of this research was to design interpolatory rational cubic splines that provide some extra degrees to control the shape of the curve, both locally and globally according to the desires of the users. This above curve methods have been generalized for 3-D object modelling.

1.5.2 Objectives

The C^2 rational interpolatory splines investigated have the following desirable properties:

1. Are capable of generating a broad range of interpolating curves

2. Are easy to implement

3. Provides shape control according to the user's wishes

4. Are computationally economical.

1.5.3 Results

1. Provides C^2 alternative to the well known existing GC^2 or C^1 methods like cubic ν-spline of [6] and weighted ν-splines of [1].

2. Have parameters associated with each control point and interval. which provides a variety of shape controls like point and interval tensions.

Chapter 2

RATIONAL SPLINES WITH INTERVAL TENSION

2.1 Introduction

A rational cubic spline with interval tension was described and analysed in [2]. It provides a C^2 computationally simpler alternative to the exponential spline under tension [7] and an alternative to C^1 and GC^2 spline methods like the weighted ν-spline [1] and γ-spline [13]. The rational cubic spline maintains the C^2 parametric continuity of the curve. rather than the more general geometric GC^2 arc length continuity achieved by the ν-spline and β-spline. Regarding shape characteristics. it has a shape control parameter associated with each interval which can be used to flatten or tighten the curve both locally and globally. Since the spline is defined on a non-uniform knot partition, the partition itself provides additional degrees of freedom on the curve. However the parameterization is normally expected to be defined on a uniform knot partition, or by cumulative chord length. or by some other appropriate means.

This chapter presents a description and analysis of a rational cubic interpolatory spline which has a shape parameter associated with each interval. The spline can be used in CAGD, to represent the parametric curves and surfaces in interpolatory form. The rational spline is based on a rational cubic Hermite interpolant. Section(2.4) describes the freeform rational spline and analyses its behavior with respect to shape parameter in each interval. Section(2.5) describes the interpolatory rational spline, with examples which illustrate the interval tension property of the rational spline. Section(2.6) and section(2.7) describe freeform and interpolatory surfaces respectively.

2.2 C^1 Rational Cubic Hermite Interpolant

A piecewise rational cubic Hermite parametric function $p \in C^1[t_0, t_n]$, with parameters r_i, $i = 0, \dots, n-1$ is defined for $t \in [t_i, t_{i+1}]$, $i = 0, \dots, n-1$, by
$p(t) = p_i(t; r_i) =$

$$\frac{(1-\theta)^3 F_i + \theta(1-\theta)^2(r_i F_i + h_i D_i) + \theta^2(1-\theta)(r_i F_{i+1} - h_i D_{i+1}) + \theta^3 F_{i+1}}{1 + (r_i - 3)\theta(1-\theta)} \tag{2.1}$$

where $r_i \geq 0.$, will be used as tension parameters to control the shape of the curve. The case $r_i = 3$, $i = 0, \dots, n-1$, is that of cubic Hermite interpolation and the restriction $r_i > -1$ ensures a positive denominator in equation(2.1).

The function $p(t)$ has the Hermite interpolation properties :

$$p(t_i) = F_i \text{ and } p^{(1)}(t_i) = D_i,\ i = 0, \ldots, n.$$

For $r_i \neq 0$, equation(2.1) can be written in the form:

$p_i(t; r_i) =$

$$R_0(\theta; r_i)F_i + R_1(\theta; r_i)V_i + R_2(\theta; r_i)W_i + R_3(\theta; r_i)F_{i+1}, \tag{2.2}$$

where

$$V_i = F_i + h_i D_i / r_i,\ W_i = F_{i+1} - h_i D_{i+1} / r_i.$$

and $R_j(\theta; r_i)$, $j = 0, 1, 2, 3$. are appropriately defined rational functions with

$$\sum_{j=0}^{3} R_j(\theta; r_i) = 1. \tag{2.3}$$

Moreover, these functions are rational Bernstein-Bezier weight functions which are non-negative for $r_i > 0$. Thus in R^N, $N > 1$ and for $r_i > 0$ the *convex hull property* holds *i.e* the curve segment P_i lies in the convex hull of the control points $\{F_i, V_i, W_i, F_{i+1}\}$. Moreover, the *variation diminishing property* also holds of the rational cubic *i.e* the curve segment p_i crosses any (hyper) plane of dimensions N-1 no more times than it crosses the control polygon joining F_i, V_i, W_i, F_{i+1}.

The rational cubic of equation(2.1) can be expressed as:

$$p_i(t; r_i) = l_i(t) + e_i(t; r_i), \text{ where}$$

$$l_i(t) = (1 - \theta)F_i + \theta F_{i+1}$$

$$e_i(t; r_i) = \frac{h_i \theta(1-\theta)[(\Delta_i - D_i)(\theta - 1) + (\Delta_i - D_{i+1})\theta]}{1 + (r_i - 3)\theta(1-\theta)}$$

This immediately leads to *Interval tension property* i.e. for given fixed (or bounded) D_i, D_{i+1}, the rational cubic Hermite interpolant of equation(2.1) converges uniformly to the linear interpolant on $[t_i, t_{i+1}]$ as $r_i \to \infty$.

In the following section, a C^2 rational spline interpolant is constructed. This requires knowledge of the 2^{nd} derivative of equation(2.1) which, after some simplification, is given by

$$p_i^{(2)}(t;r_i) = \frac{2\{\alpha_i\theta^3 + \beta_i\theta^2(1-\theta) + \gamma_i\theta(1-\theta)^2 + \delta_i(1-\theta)^3\}}{h_i\{1+(r_i-3)\theta(1-\theta)\}^3} \tag{2.4}$$

where

$$\alpha_i = r_i(D_{i+1} - \Delta_i) - D_{i+1} + D_i$$
$$\beta_i = 3(D_{i+1} - \Delta_i)$$
$$\gamma_i = 3(\Delta_i - D_i)$$
$$\delta_i = r_i(\Delta_i - D_i) - D_{i+1} + D_i$$

2.3 C^2 Rational Cubic Spline Interpolant

We now follow the familiar procedure of allowing the derivative parameters D_i, $i = 0, \ldots, n$ to be degrees of freedom which are constrained by the imposition of the C^2 continuity conditions

$$p^{(2)}(t_{i+}) = p^{(2)}(t_{i-}),\ i = 1, \ldots, n-1. \tag{2.5}$$

These C^2 conditions give, from equation(2.4), the linear system of consistency equations.

$$h_i D_{i-1} + \{h_i(r_{i-1} - 1) + h_{i-1}(r_i - 1)\} D_i + h_{i-1} D_{i+1} \tag{2.6}$$
$$= h_i r_{i-1} \Delta_{i-1} + h_{i-1} r_i \Delta_i, \quad i = 1, \ldots, n-1$$

For simplicity , assume that D_0 and D_n are given as end conditions (clearly other end conditions are also appropriate.). Assume also that

$$r_i \geq r > 2, \; i = 0, \ldots, n-1$$

Then the equation(2.6) defines a diagonally dominant, tri-diagonal linear system in the unknowns D_i, $i = 1, \ldots, n-1$. Hence there exists a unique solution which can be easily calculated by use of the tri-diagonal LU decomposition algorithm. Thus a rational cubic spline interpolant can be constructed with tension parameters r_i, $i = 0, \ldots, n-1$, where the special case $r_i = 3$, $i = 0, \ldots, n-1$, is that of cubic spline interpolation.

2.4 Rational Cubic Spline with Interval Tension

This section reviews the rational spline with tension (B-spline representation) method [2]. For the purpose of the analysis, let additional knots be introduced outside the interval $[t_0, t_n]$, defined by $t_{-3} < t_{-2} < t_{-1} < t_0$ and $t_n < t_{n+1} < t_{n+2} < t_{n+3}$. Let

$$r_i \geq r > 2, \; i = -3, \ldots, n+2 \tag{2.7}$$

be shape parameters defined on this extended partition. Rational cubic spline functions ψ_j, $j = -1, \ldots, n+3$, have been constructed, see Figure 2.1(a), such that

$$\psi_j(t) = 0, \quad \text{for} \quad t < t_{j-2} \tag{2.8}$$

$$\psi_j(t) = 1, \quad \text{for} \quad t \geq t_{j+1}$$

The local support rational cubic B-spline basis, see Figure 2.1(c) is now defined by the difference functions:

$B_j(t) = \psi_j(t) - \psi_{j+1}(t), \quad j = -1, \ldots, n+1$

Let $R_k(\theta; r_i)$, $k = 0, 1, 2, 3$ be defined as :

$$R_0(\theta; r_i) = (1-\theta)^3 / Q_0(\theta; r_i),$$

$$R_1(\theta; r_i) = r_i \theta (1-\theta)^2 / Q_0(\theta; r_i),$$

$$R_2(\theta; r_i) = r_i \theta^2 (1-\theta) / Q_0(\theta; r_i),$$

$$R_3(\theta; r_i) = \theta^3 / Q_0(\theta; r_i)$$

where $\quad Q_0(\theta; r_i) = 1 + (r_i - 3)\theta(1-\theta).$

A local support rational cubic B-spline basis $B_j(t)$, $j = -1, \ldots, n+1$ was constructed and an explicit representation was given as:

$$B_j(t) = R_0(\theta; r_i) B_j(t_i) + R_1(\theta; r_i)(B_j(t_i) + h_i B_j^{(1)}(t_i)/r_i) + \tag{2.9}$$

$$R_2(\theta; r_i)(B_j(t_{i+1}) - h_i B_j^{(1)}(t_{i+1})/r_i) + R_3(\theta; r_i) B_j(t_{i+1}).$$

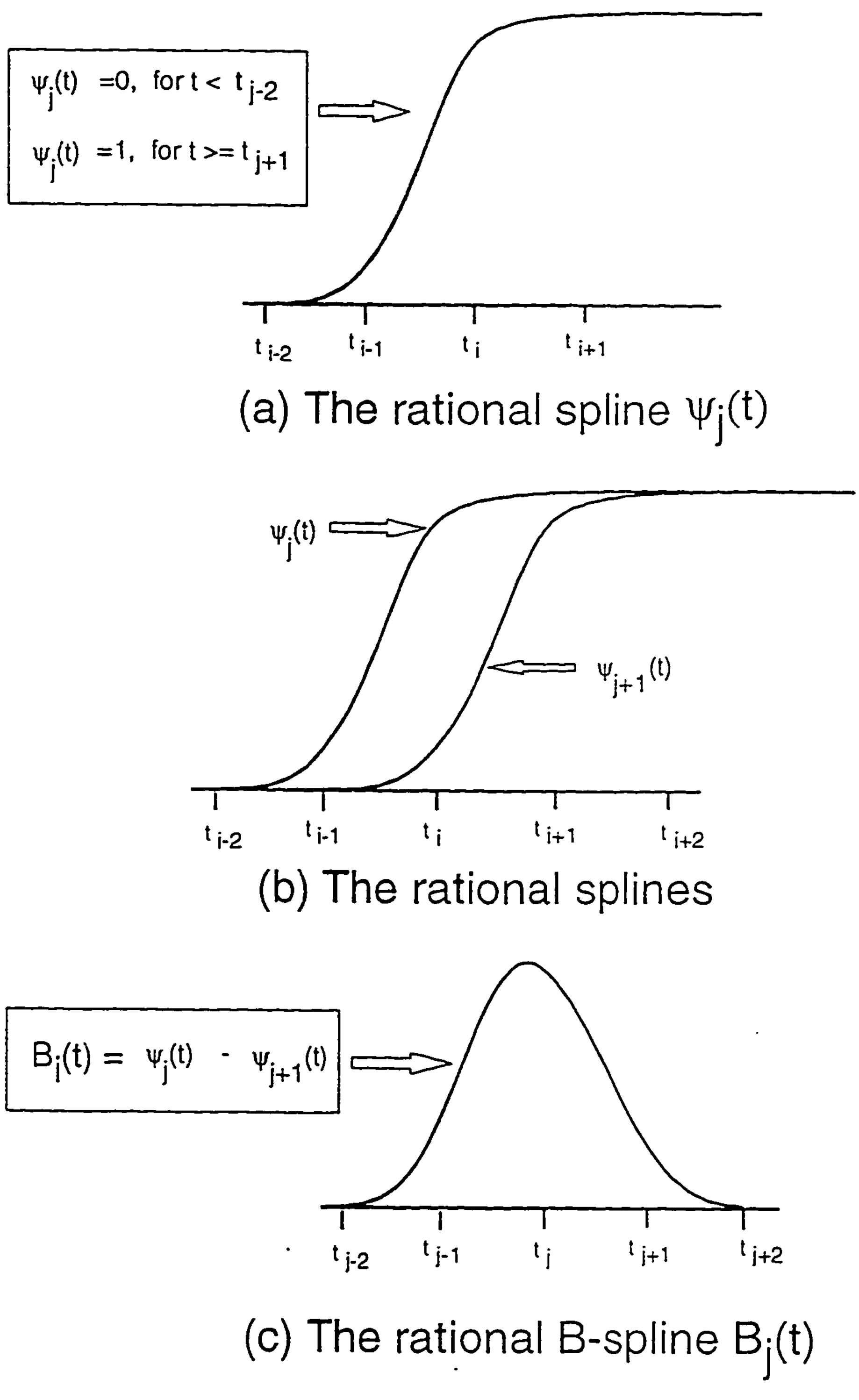

Figure 2.1: The rational spline forms

where

$$B_j(t_i) = B_j^{(1)}(t_i) = 0, \quad \text{for } \; i \neq j-1, j, j+1 \tag{2.10}$$

and

$$\begin{aligned} B_j(t_{j-1}) &= \mu_{j-1}, \quad B_j^{(1)}(t_{j-1}) = \hat{\mu}_{j-1}, \\ B_j(t_j) &= 1 - \lambda_j - \mu_j, \quad B_j^{(1)}(t_j) = \hat{\lambda}_j - \hat{\mu}_j, \\ B_j(t_{j+1}) &= \lambda_{j+1}, \quad B_j^{(1)}(t_{j+1}) = -\hat{\lambda}_{j+1} \end{aligned} \tag{2.11}$$

with

$$\begin{aligned} \lambda_j &= h_j \hat{\lambda}_j / r_j, \quad \mu_j = h_{j-1} \hat{\mu}_j / r_{j-1} \\ \hat{\lambda}_j &= h_j d_{j-1} / c_j, \quad \hat{\mu}_j = h_{j-1} d_{j+1} / c_{j+1}, \\ c_j &= h_{j-2} d_j \left(\frac{h_{j-2}}{r_{j-2}} + \frac{h_{j-1}}{r_{j-1}}\right) + h_j d_{j-1} \left(\frac{h_{j-1}}{r_{j-1}} + \frac{h_j}{r_j}\right) + \\ &\qquad \frac{h_{j-1} d_{j-1} d_j}{r_{j-1}}, \\ d_j &= h_j (r_{j-1} - 2) + h_{j-1} (r_j - 2). \end{aligned}$$

These rational spline functions, see Figure 2.1, are such that

1. (local support) $B_j(t) = 0$, for $t \in (t_{j-2}, t_{j+2})$.

2. (Partition of unity) $\sum_{j=-1}^{n+1} B_j(t) = 1$, for $\; t \in [t_0, t_n]$

3. (Positivity) $B_j(t) \geq 0$, for all t,

and hence enjoy all the B-spline properties.

The design curve is given by:

$$p(t) = \sum_{j=-1}^{n+1} P_j B_j(t), \ t \in [t_0, t_n] \tag{2.12}$$

where $P_j \in R^N$ define the control points, was transformed to the piecewise defined rational Bernstein-Bezier representation, see Figure 2.2 :

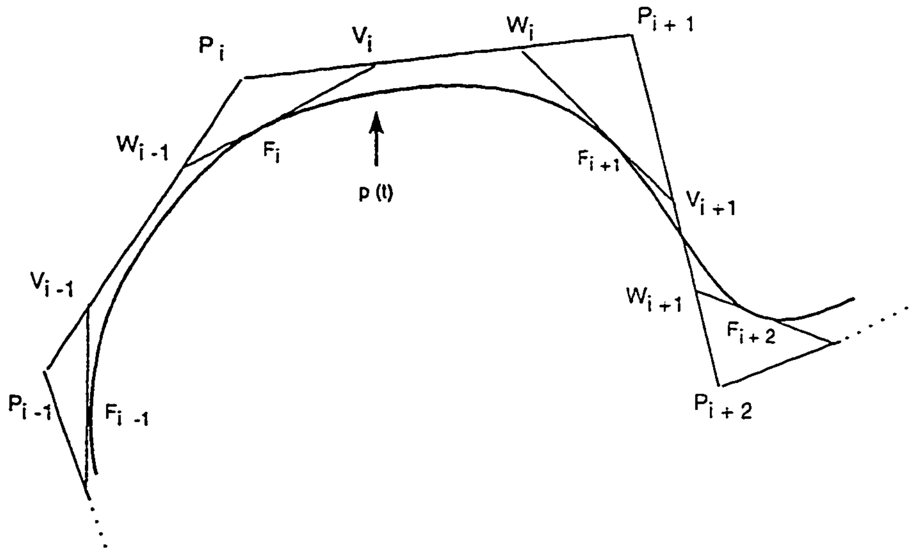

Figure 2.2: Rational Bernstein-Bezier representation

$$p(t) = R_0(\theta; r_i)F_i + R_1(\theta; r_i)V_i + R_2(\theta; r_i)W_i + R_3(\theta; r_i)F_{i+1}, \tag{2.13}$$

where

$$P_{i-1}\lambda_i + P_i(1-\lambda_i-\mu_i) + P_{i+1}\mu_i = F_i \tag{2.14}$$
$$(1-\alpha_i)P_i + \alpha_i P_{i+1} = V_i$$
$$\beta_i P_i + (1-\beta_i)P_{i+1} = W_i$$

with

$$\alpha_i = \mu_i + h_i\hat{\mu}_i/r_i \tag{2.15}$$
$$\beta_i = \lambda_{i+1} + h_i\hat{\lambda}_{i+1}/r_i$$

Let

$$X_i=[F_i\ V_i\ W_i\ F_{i+1}]^T,\ Z_i = [P_{i-1}\ P_i\ P_{i+1}\ P_{i+2}]^T$$

and

$$Y_i = \begin{bmatrix} \lambda_i & 1-\lambda_i-\mu_i & \mu_i & \\ & 1-\alpha_i & \alpha_i & \\ & \beta_i & 1-\beta_i & \\ & \lambda_{i+1} & 1-\lambda_{i+1}-\mu_{i+1} & \mu_{i+1} \end{bmatrix} \tag{2.16}$$

Then the transformation of equation(2.14) can also be represented in matrix notation as

$$X_i = Y_i.Z_i \tag{2.17}$$

The transformation to rational Bernstein-Bezier form is very convenient for computational purposes and also leads to:

1. **Variation diminishing property:** The rational B-spline curve $p(t)$, $t \in$

$[t_0, t_n]$, defined by equation(2.12), crosses any (hyper) plane of dimension N-1 no more times than it crosses the control polygon P joining the control points $\{P_j\}_{=-1}^{n+1}$, see Figure 2.3 .

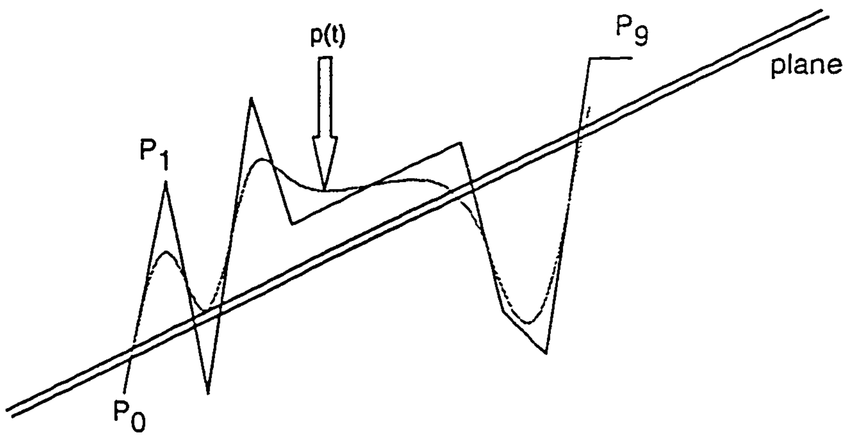

Figure 2.3: Variation diminishing property

2. **Global tension property:** Let $r_i \geq r > 2$, $i = -2, \ldots, n+1$, and let P denote the rational B-spline control polygon, defined explicitly on $[t_i, t_{i+1}]$, $i = -1, \ldots, n$ by

$$P(t) = (1-\theta)P_i + \theta P_{i+1}, \tag{2.18}$$

then the rational B-spline representation (2.12) converges uniformly on $[t_{-1}, t_{n+1}]$ as $r \rightarrow \infty$, see Figure 2.4(a)

3. **Interval tension property:** Consider an interval $[t_k, t_{k+1}]$ for a fixed $k \in \{0, \ldots, n-1\}$ and let

$$Q_k = (1-\mu)P_k + \mu P_{k-1},$$

$$Q_{k+1} = \lambda P_k + (1 - \lambda)P_{k+1}$$

denote two distinct points on the line segment of the control polygon joining P_k, P_{k+1}, where

$$\lambda = \frac{h_{k+1}/r_{k+1}}{(h_{k-1}/r_{k-1} + h_{k+1}/r_{k+1} + h_k)}$$
$$\mu = \frac{h_{k-1}/r_{k-1}}{(h_{k-1}/r_{k-1} + h_{k+1}/r_{k+1} + h_k)}$$

Then the rational B-spline representation of equation(2.12) converges uniformly to Q, see Figure 2.4(b) on $[t_k, t_{k+1}]$ as $r_k \rightarrow \infty$, where

$$Q(t) = (1 - \theta)Q_k + \theta Q_{k+1} \tag{2.19}$$

Figure 2.5(a) and Figure 2.5(b) illustrate the interval tension behavior of the curves. As the value of r_k and r_{k+1} increases the resulting curve segment approaches the line segment P_k, P_{k+1}.

For the proof of the above properties the reader is referred to [14]

2.5 Interpolatory Rational Spline with Interval Tension

In interpolatory case we are given a set of data points $F_0, F_1, \ldots, F_n$. We want a cubic B-spline curve p determined by unknown control vertices $P_{-1}, P_0, \ldots, P_{n+1}$, such that $p(t_i) = F_i$ in other words, p interpolates to the data points. The process of obtaining the interpolatory rational cubic B-spline with interval shape control is

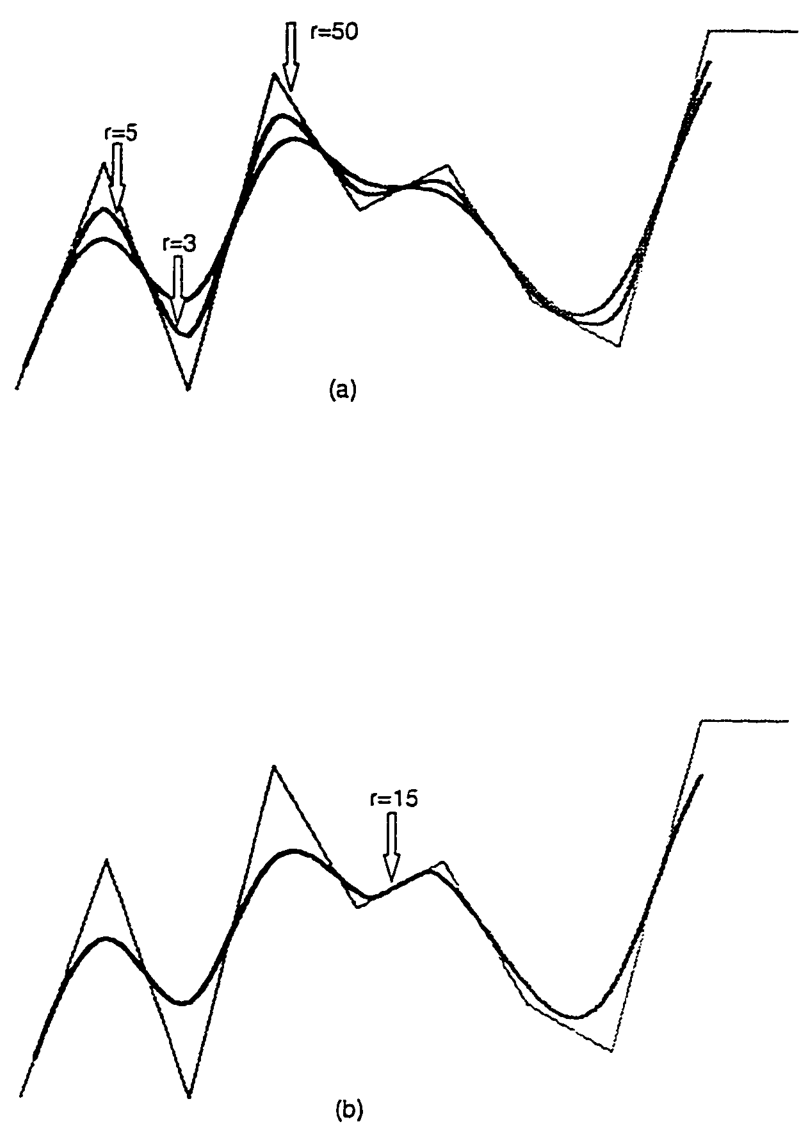

Figure 2.4: Global/local tension properties of rational B-splines

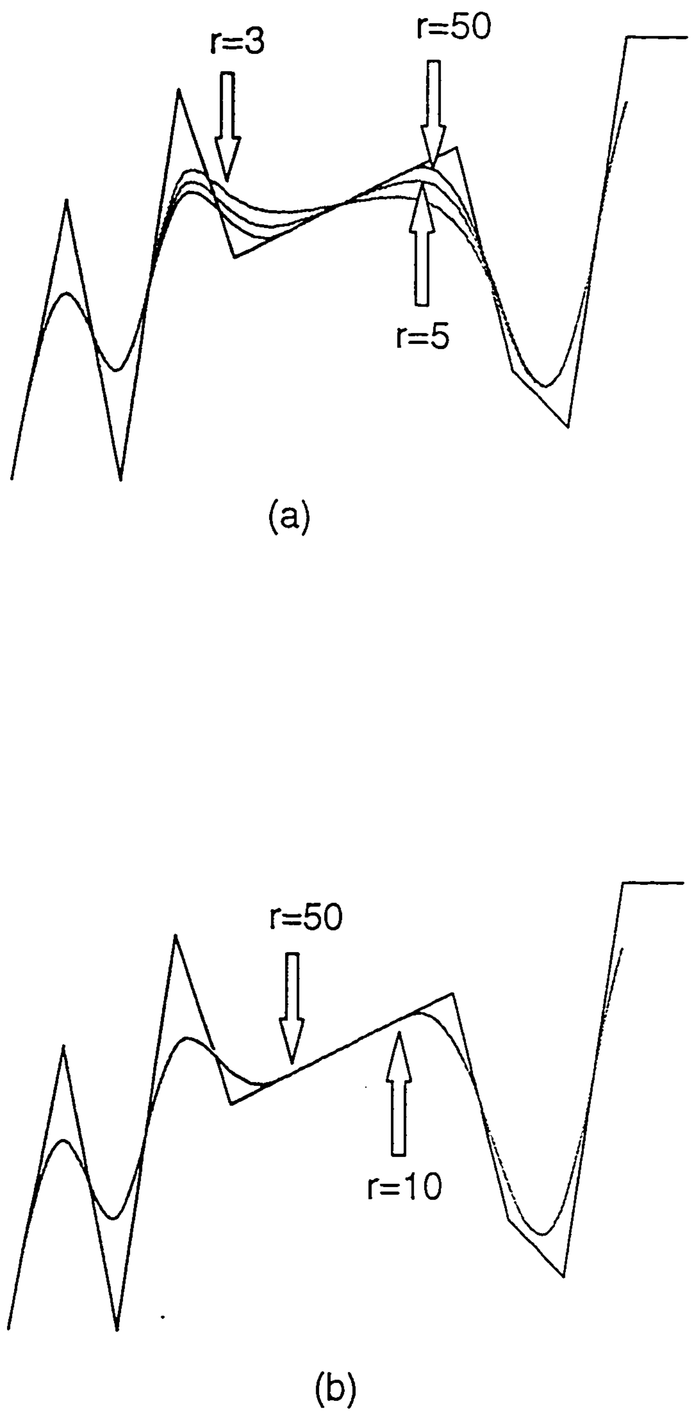

Figure 2.5: Local tension properties of rational B-splines

accomplished through

$$\sum_{j=-1}^{n+1} P_j B_j(t) = F_i, \; \forall\, i \tag{2.20}$$

where the matrix $B_j(t)$ is the tridiagonal matrix. From equation(2.14) F_i's, i = $0, \ldots, n$ can be written as

$$F_i = P_{i-1}\lambda_i + P_i(1 - \lambda_i - \mu_i) + P_{i+1}\mu_i \tag{2.21}$$

$$T.P = F \tag{2.22}$$

The above set of equations for F_i, $i = 0, \ldots, n$. i.e the given set of data points, through which the resulting curve must pass, and the control points P's can be written as in equation(2.22). The values of F, P and T are as shown below. As such the above system is underdefined and for a unique solution we need to specify two further conditions, one at the start and one at the end of the curve. We shall repeat the two end control points, although it is not the only end condition available. The above system of equations is tridiagonal- only the diagonal elements and the two neighbors are nonzero. By exploiting the structure of the tridiagonal matrix we can solve the resulting system of equations more efficiently and bypass the standard elimination techniques.

$$
T = \begin{bmatrix}
1-\lambda_1-\mu_1 & \mu_1 & & & & \\
\lambda_2 & 1-\lambda_2-\mu_2 & \mu_2 & & & \\
& \lambda_3 & 1-\lambda_3-\mu_3 & \mu_3 & & \\
& & \lambda_4 & 1-\lambda_4-\mu_4 & \mu_4 & \\
& & & & & \\
& & & & \lambda_n & 1-\lambda_n-\mu_n
\end{bmatrix}
$$

$$
P = \begin{bmatrix} P_0 \\ P_1 \\ P_2 \\ . \\ . \\ . \\ P_{n-1} \\ P_n \end{bmatrix} \qquad F = \begin{bmatrix} F_0 \\ F_1 \\ F_2 \\ . \\ . \\ . \\ F_{n-1} \\ F_n \end{bmatrix}
$$

From equation(2.22) we get

$$P = T^{-1}.F \tag{2.23}$$

That is the control vertices of the curve which passes through the given data points F_i's are given by the P_i's as in equation(2.23). When these values of P_i's are substituted in equation(2.12), we get the required C^2 interpolatory B-spline curve with interval tension.

2.5.1 Examples:

The shape behavior of the interpolatory rational spline with interval tension are illustrated by the following simple examples for the data set in R^2. The global tension behavior is shown in Figure 2.6, where all shape parameters are progressively increased with values 3, 7, and 50. The effect of the high interval tension is clearly seen in that the resulting spline curve in Figure 2.6(c) approaches the control polygon. Figure 2.7(b) and Figure 2.7(c) display the interval tension behavior applied to the curve of Figure 2.6(a).

2.6 Freeform Rational B-Spline Surfaces

In this section we generalize the idea of section(2.4) to surfaces.

2.6.1 Rational B-Splines and the Design Surface

Suppose that we are given points

$$P_{i,j} \in R^3,\ i = -1, \ldots, m+1,\ j = -1, \ldots, n+1 \tag{2.24}$$

and knot sequences

$$\tilde{t}_o < \tilde{t}_1 < \ldots < \tilde{t}_m$$

$$t_o < t_1 < \ldots < t_n$$

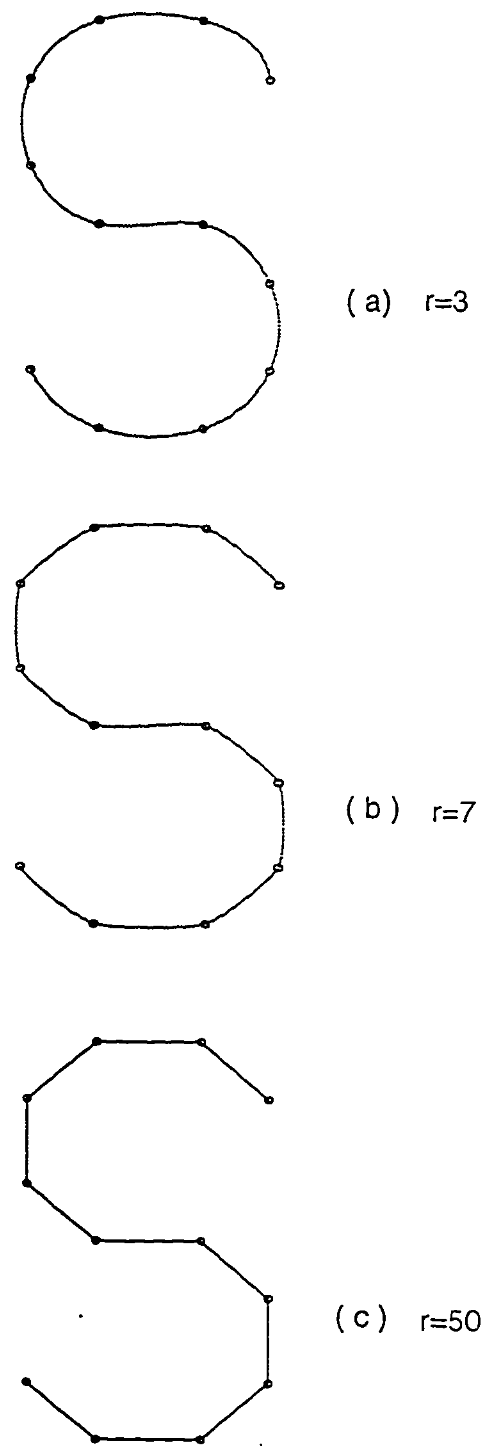

Figure 2.6: Interpolatory curves, with global tension

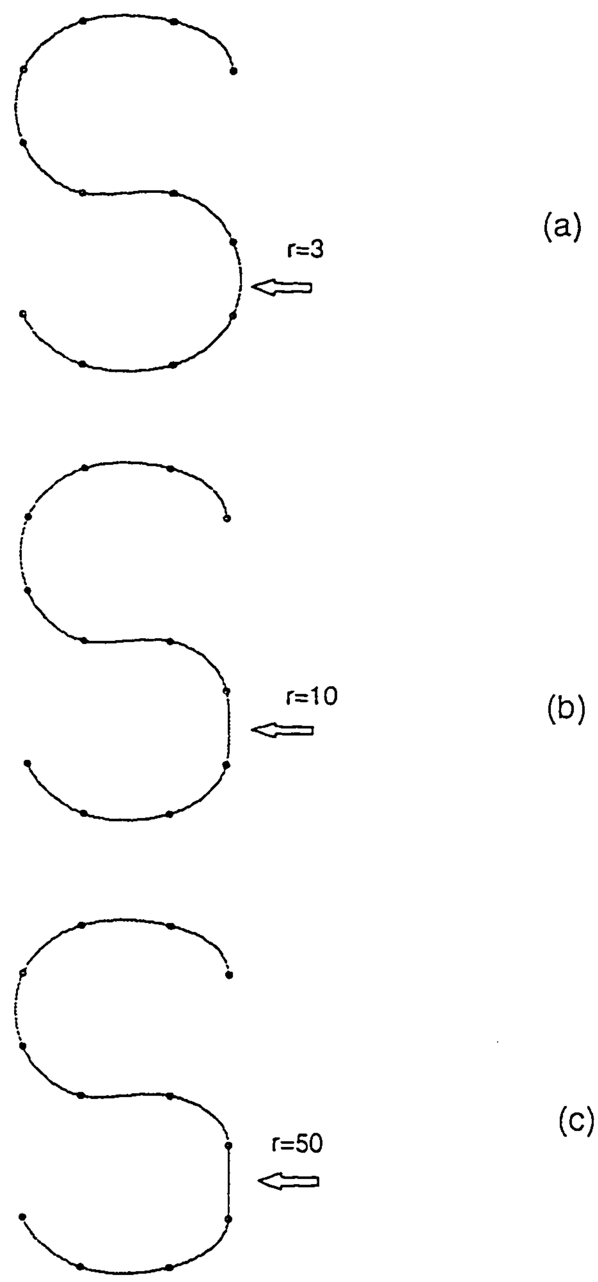

Figure 2.7: Interpolatory curves, with local tension

with appropriate additional knots

$$\tilde{t}_{-3} < \tilde{t}_{-2} < \tilde{t}_{-1} < \tilde{t}_0; \quad \tilde{t}_m < \tilde{t}_{m+1} < \tilde{t}_{m+2} < \tilde{t}_{m+3}.$$
$$t_{-3} < t_{-2} < t_{-1} < t_0; \quad t_n < t_{n+1} < t_{n+2} < t_{n+3}$$

We need to find a parametric rational B-spline surface $p(\tilde{t}, t)$ in such a way that $p(\tilde{t}, t_j)$ and $p(\tilde{t}_i, t)$ are freeform rational cubic splines with tension in $\tilde{t}$– and t-directions for all i and j respectively.

Suppose we are given tension parameters

$$\tilde{r}_{i,j} > 2 \text{ and } r_{i,j} > 2, \ i = -3, \ldots, m+2, \ j = -3, \ldots, n+2, \tag{2.25}$$

with $\tilde{B}_k(\tilde{t}, t)$ and $B_l(t, \tilde{t})$ the corresponding rational B-spline basis functions, as in section(2.4) but with variable cubic B-spline tensions $\tilde{r}_i(t)$ and $r_j(\tilde{t})$ defined as:

$$\tilde{r}_i(t) = \sum_j \tilde{r}_{i,j} N_j(t), \tag{2.26}$$
$$r_j(\tilde{t}) = \sum_i r_{i,j} N_i(\tilde{t})$$

where $N_j(t)$'s are cubic B-splines. These can be computed as a special case of the rational cubic splines of section(2.4).

Remark: The convex hull property of N_j and equation(2.25) show that $\tilde{r}_i(t)$, $r_j(\tilde{t}) > 2$, $\forall$ i, j, t, and $\tilde{t}$. Also, for any j

$$\tilde{r}_i(t) = 0, \ t \notin (t_{j-2}, t_{j+2})$$

and for any i

$$r_j(\tilde{t}) = 0, \ \tilde{t} \notin (t_{i-2}, \ t_{i+2})$$

Furthermore, a large value of the shape parameter $\tilde{r}_{i,j}$ for any j results in large values of $\tilde{r}_i(t)$ in the intervals $[t_{j-1}, t_j]$, $[t_j, t_{j+1}]$ and $[t_j, t_{j+1}]$. A similar characteristic is possessed by $r_j(\tilde{t})$. Thus a sufficiently large value of any of the shape parameters in equation(2.25) (for $i = 0, \ldots, m-1$, $j = 0, \ldots, n-1$) results in a sufficiently large value of the variable weight in the corresponding interval. In particular, if any of $\tilde{r}_{i,j}$ and $r_{i,j}$, $i = 0, \ldots, m-1$, $j = 0, \ldots, n-1$ tend to infinity, it causes the corresponding values from amongst $\tilde{r}_i(t_j)$ and $r_j(\tilde{t}_i)$, $i = 0, \ldots, m-1$, $j = 0, \ldots, n-1$ respectively to approach infinity. Hence the shape parameters in equation(2.25) are chosen in such a way that one shape parameter is associated with each interval.

The surface by local support property is defined as:

$$p(\tilde{t}, t) = \sum_{k=i-1}^{i+2} \sum_{l=j-1}^{j+2} P_{k,l} \tilde{B}_k(\tilde{t}, t) B_l(t, \tilde{t}) \tag{2.27}$$

where $\tilde{t}_i \leq \tilde{t} < \tilde{t}_{i+1}$: $t_j \leq t < t_{j+1}$, $i = 0, \ldots, m-1$, $j = 0, \ldots, n-1$

Substitution of the Bernstein-Bezier form of the rational B-splines gives the piecewise defined rational Bernstein-Bezier representation:

$$p(\tilde{t}, t) = \sum_{k=0}^{3} \sum_{l=0}^{3} X_{k,l}^{i,j}(\tilde{t}, t) R_k(\tilde{\theta}; \tilde{r}_i(t)) R_l(\theta; r_j(\tilde{t})). \tag{2.28}$$

where the Bernstein-Bezier points $X_{k,l}^{i,j}(\tilde{t}, t)$ can be computed from the rational B-spline vertices $P_{i,j}$ as

$$X_{i,j} = \tilde{Y}_i . Z_{i,j} . Y_j^T \tag{2.29}$$

where

$$X_{i,j} = \begin{bmatrix} X^{i,j}_{0,0} & X^{i,j}_{0,1} & \dots & X^{i,j}_{0,3} \\ X^{i,j}_{1,0} & \dots & \dots & \dots \\ \dots & \dots & \dots & \dots \\ X^{i,j}_{3,0} & \dots & \dots & X^{i,j}_{3,3} \end{bmatrix}$$

$$Z_{i,j} = \begin{bmatrix} P_{i-1,j-1} & P_{i-1,j} & \dots & P_{i-1,j+2} \\ P_{i,j-1} & .. & \dots & \dots \\ \dots & \dots & \dots & \dots \\ P_{i+2,j-1} & \dots & & P_{i+2,j+2} \end{bmatrix}$$

and the matrix Y_j is given as in equation(2.16) as well as $\tilde{Y}_i$ provided tildes are put where appropriate. $\tilde{Y}_i$ and Y_j^T now depend on $\tilde{t}$ and t respectively.

2.6.2 Tension Properties

The rational B-spline surface representation equation(2.28) satisfies the *global tension* property and the *local tension* property as proved in [14].

2.7 Interpolatory Rational B-Spline Surfaces

Expanding equation(2.29) we get the points through which the freeform rational B-spline surface passes, for given control points say P's. Here in our case we need to find P's (the new control points) given the data points F's, through which the interpolatory rational B-spline surface should pass. Let us denote it by F:

$$F_{i,j} = X = \tilde{\lambda}_i[P_{i-1,j-1}\lambda_j + P_{i-1,j}(1-\lambda_j-\mu_j) + P_{i-1,j+1}\mu_j] + \tag{2.30}$$

$$(1 - \tilde{\lambda}_i - \tilde{\mu}_i)[P_{i,j-1}\lambda_j + P_{i,j}(1 - \lambda_j - \mu_j) + P_{i,j+1}\mu_j] +$$
$$\tilde{\mu}_i[P_{i+1,j-1}\lambda_j + P_{i+1,j}(1 - \lambda_j - \mu_j) + P_{i+1,j+1}\mu_j]$$

For $i = 1, \ldots, n$ and $j = 1, \ldots, m$:

We can observe from the above that the sum of the coefficients of P's equal to unity. Which means that the resulting interpolatory surface satisfies the *convex hull property*. Let

$$A_{i,j} = P_{i,j-1}\lambda_j + P_{i,j}(1 - \lambda_j - \mu_j) + P_{i,j+1}\mu_j \tag{2.31}$$

Equation(2.30) can be expressed as :

$$F = T.A \tag{2.32}$$

where F. T. and A are as given below:

$$T = \begin{bmatrix} 1-\hat{\lambda}_1-\hat{\mu}_1 & \hat{\mu}_1 & & & & & \\ \hat{\lambda}_2 & 1-\hat{\lambda}_2-\hat{\mu}_2 & \hat{\mu}_2 & & & & \\ & \hat{\lambda}_3 & 1-\hat{\lambda}_3-\hat{\mu}_3 & \hat{\mu}_3 & & & \\ & & \hat{\lambda}_4 & 1-\hat{\lambda}_4-\hat{\mu}_4 & \hat{\mu}_4 & & \\ & & & & & & \\ & & & & & & \\ & & & & & \hat{\lambda}_m & 1-\hat{\lambda}_m-\hat{\mu}_m \end{bmatrix}$$

$$A=\begin{bmatrix} A_{1,1} \\ A_{2,1} \\ . \\ . \\ \\ A_{m-1,1} \\ A_{m,1} \end{bmatrix} \quad \text{and} \quad F=\begin{bmatrix} F_{1,1} \\ F_{2,1} \\ \\ . \\ . \\ F_{m-1,1} \\ F_{m,1} \end{bmatrix}$$

Since T is invertible. we get from equation(2.32)

$$A = T^{-1}.F \tag{2.33}$$

Moreover. from equation(2.31) A can be expressed as:

$$A = D.P \tag{2.34}$$

The values of A, P, and D are as given below:

$$D = \begin{bmatrix} 1-\lambda_1-\mu_1 & \mu_1 & & & \\ \lambda_2 & 1-\lambda_2-\mu_2 & \mu_2 & & \\ & \lambda_3 & 1-\lambda_3-\mu_3 & \mu_3 & \\ & & \lambda_4 & 1-\lambda_4-\mu_4 & \mu_4 \\ & . & & & \\ & & . & & \\ & & & \lambda_n & 1-\lambda_n-\mu_n \end{bmatrix}$$

$$A = \begin{bmatrix} A_{i,1} \\ A_{i,2} \\ . \\ . \\ A_{i,n-1} \\ A_{i,n} \end{bmatrix} \quad \text{and} \quad P = \begin{bmatrix} P_{i,1} \\ P_{i,2} \\ . \\ P_{i,n-1} \\ P_{i,n} \end{bmatrix}$$

The process of calculating the new control points P's. is carried out in two stages, first the entire matrix A is calculated. Then the new control points P's can be calculated as

$$P = D^{-1}..A \tag{2.35}$$

which when substituted in equation(2.28), gives the required interpolatory surface with interval tension which can be controlled both locally and globally.

2.7.1 Examples

Consider a set of three dimensional data. The figures show the effect of increase in tensions, both locally and globally. The Figure 2.8(a) is the control net. Surface in Figure 2.8(b) corresponds to the value $r = \hat{r} = 3$ (the bicubic case). Surface in Figure 2.9(a) converges to the control polyhedron as $r = \hat{r} = 50$. The local change of tension parameters is evident in Figure 2.9(b).

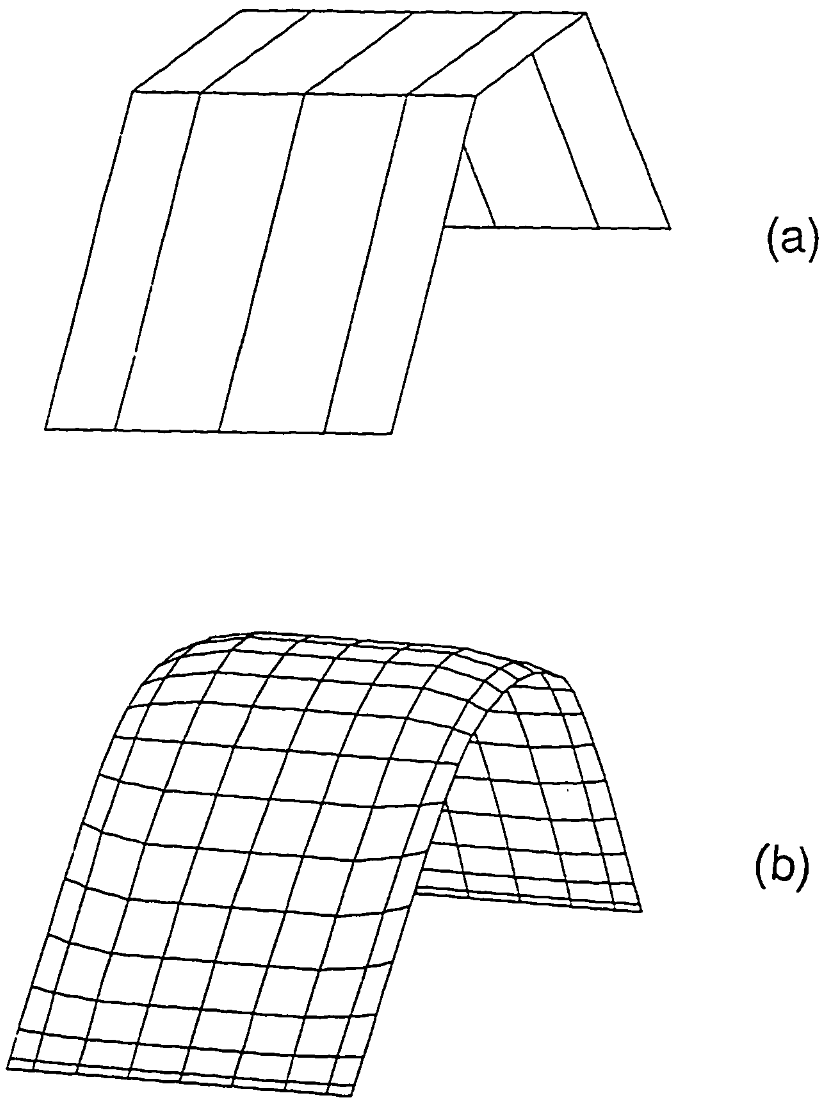

Figure 2.8: Interpolatory surfaces, with interval tension

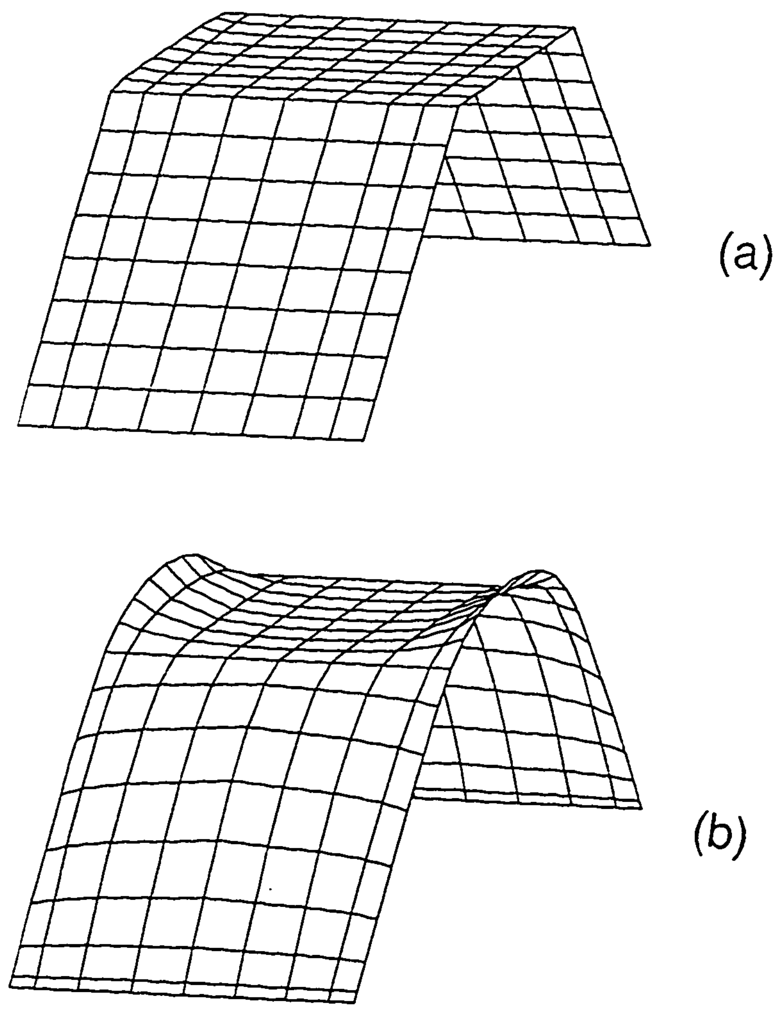

Figure 2.9: Interpolatory surfaces, with interval tension

2.8 Concluding Remarks

An analysis of a rational cubic tension spline has been developed with a view to its application in CAGD. We have found it appropriate to construct a rational form which involves just one tension parameter per interval, although clearly the rational form defined by equation(2.1) could be generalized. One advantage of the use of C^2 parametric continuity, compared with that of the more general geometric GC^2 continuity, becomes apparent in the application of such a rational spline method for surfaces. In this case we followed the approach of [15], in the use of the spline blended methods of [16]. Nielson proposes a spline blended surfaces of GC^2 curves. However, the use of parametric C^2 curves in the blend will alleviate this loss of continuity.

The idea of C^2 freeform rational B-spline is extended to achieve a C^2 interpolatory parametric rational B-spline which can be controlled locally and globally. For CAGD applications, the developed interpolatory spline provides a parameter to control the shape of a curve on each interval. The surface has been designed through the sum of the products of bivariate rational B-spline basis functions. The use of variable tensions allows shape control. This is not a tensor product surface but a tensor product surface can be recovered as a special case. This is not a NURBS representation either: the NURBS representation of the surface has some limitations regarding its shape control. Computation of the surface has been suggested through the Bernstein-Bezier representation which is quite convenient.

Chapter 3

RATIONAL SPLINES WITH POINT TENSION

3.1 Introduction

Interactive designing of the curves and surfaces is a common problem of CAD, CAM, Solid Modelling and Graphics today. It is typically accomplished through the manipulation of a control polygon. The approach based on B-spline type basis functions results in a curve that lies in the convex hull. Changes in the control polygon only affect the curve locally. The alternative approach based upon interpolating the curve passes a spline type curve through the control points. A change in a single control point can affect the entire curve. Both approaches are useful and it is desirable to introduce a class of curves and associated techniques that allows not only either style of interaction but also has the capability to control the shape of the curves and corresponding rectangular surfaces, locally and globally, according to the desires of the user. This chapter is oriented towards the B-spline type approach, for the representation of curves and surfaces, using rational cubic splines.

B-splines are a useful and powerful tool for CAGD and Solid Modelling, and they can be found frequently in the existing CAD/CAM systems. They form a basis for the space of n^{th} degree splines of continuity class C^{n-1}. Each B-spline is a non-negative n^{th} degree spline that is non-zero only on $n+1$ intervals. The B-splines form a partition of unity, that is, they sum up to one. Curves generated by summing control points multiplied by the B-splines have some very desirable shape properties, including the local *convex hull* property and *variation diminishing* property.

It is still desirable to generalize the idea of B-spline like local basis functions for the classes of rational splines, with shape parameters considered in their descriptions. In this chapter a B-spline like local basis for designing of a freeform rational spline, with point tension to produce shape control both locally and globally, has been reviewed, and extended to design interpolatory curves and surfaces with point tension having shape control both locally and globally. This method uses the cubic by quadratic functions and, for given control points, constructs the freeform spline method which enjoys all the geometric properties of B-splines. Moreover, the spline representation has extra features that it is, like NURBS, is not a spline over spline form and its denominator is a quadratic term instead of a cubic. This generation of freeform rational spline curves has parameters to control the shape freely. The design curve maintains the C^2 parametric continuity. Freeform and interpolatory structure of the rational spline can not only manage to be a smoother alternative to the well known useful methods with geometric continuities, including ν-splines of

Nielson [6] and gamma splines of Boehm [13], but it is also an economical alternative to NURBS of degree 3 as it has quadratic denominator.

3.2 Rational Cubic Spline with Point Tension

In [17] a rational cubic spline with point tension was constructed by using a C^1 piecewise rational cubic Hermite parametric function

$$S_i(t) = \frac{A + B}{C} \tag{3.1}$$

where

$$A = (1-\theta)^3 v_i \mathbf{F}_i + \theta(1-\theta)^2(2+v_i)V_i$$
$$B = \theta^2(1-\theta)(2+v_{i+1})W_i + \theta^3 v_{i+1} F_{i+1}$$
$$C = (1-\theta)^2 v_i + 2\theta(1-\theta) + \theta^2 v_{i+1}$$

Where $0 \le \theta \le 1$

And we assume that the shape parameters $v_i, v_{i+1} > 0, \ \forall\ i$

This can be further expressed as :

$$S_i(t) = R_0(\theta)F_i + R_1(\theta)V_i + R_2(\theta)W_i + R_3(\theta)F_{i+1} \tag{3.2}$$

where the basis functions $R_j(\theta)$, $j = 0, \ldots, 3$ are Bernstein Bezier weight functions dependent on v_i, v_{i+1} in the interval $[t_i, t_{i+1}]$. The C^2 rational cubic spline interpolant is obtained by imposition of the C^2 continuity conditions.

In [18] an alternate to NURBS of degree three has been proposed, (henceforth referred to as ANURBS), by converting the interpolatory rational spline with point tension of [17]. The method for evaluating this rational cubic B-spline curve is suggested by a transformation to Bernstein-Bezier form. A tensor product of the above spline curves gives a rational bicubic B-spline surface.

3.2.1 A Comparative Study of NURBS and ANURBS

1. Both NURBS and ANURBS possess convex hull, variation diminishing and partition of unity properties.

2. NURBS is of spline over spline form whereas ANURBS is a single spline in its nature.

3. NURBS has cubic numerator and denominator whereas ANURBS belong to the class of splines having cubic numerator and quadratic denominator.

4. Both of them belong to the same continuity class of functions i.e C^2.

5. Both of them can be transformed into Bernstein-Bezier form. Hence the existing efficient computational methods can be implemented.

6. The rate of sharpness of ANURBS regarding the shape control is much faster than that of NURBS.

3.3 Local Support Basis

In [18] the local support rational B-spline was constructed as

$$B_j(t) = R_0(\theta)F_{j,i} + R_1(\theta)V_{j,i} + R_2(\theta)W_{j,i} + R_3(\theta)F_{j,i+1} \tag{3.3}$$

in any interval $[t_i, t_{i+1}]$. These rational spline functions are such that

1. (local support) $B_j(t) = 0$, for $t \in (t_{j-2}, t_{j+2})$,

2. (Partition of unity) $\sum_{j=-1}^{n+1} B_j(t) = 1$, for $t \in [t_0, t_n]$

3. (Positivity) $B_j(t) \geq 0$, for all t,

And hence enjoy all the B-spline properties.

To apply the rational cubic B-spline as a practical method for the curve design, a convenient method for computing the curve representation is given by:

$$S(t) = \sum_{j=-1}^{n+1} P_j B_j(t), \quad t \in [t_0, t_n] \tag{3.4}$$

where $P_j \in R^N$ define the control points.

Substitution of equation(3.3) then gives the piecewise defined rational Bernstein-Bezier representation.

$$S_i(t) = R_0(\theta)F_i + R_1(\theta)V_i + R_2(\theta)W_i + R_3(\theta)F_{i+1} \tag{3.5}$$

where

$$P_{i-1}\lambda_i + P_i(1 - \lambda_i - \mu_i) + P_{i+1}\mu_i = F_i \tag{3.6}$$

$$(1 - \alpha_i)P_i + \alpha_i P_{i+1} = V_i$$

$$\beta_i P_i + (1 - \beta_i)P_{i+1} = W_i$$

where α_i and β_i are variables dependent on parameters θ and v. Let

$$X_i=[F_i\ V_i\ W_i\ F_{i+1}]^T,\ Z_i = [P_{i-1}\ P_i\ P_{i+1}\ P_{i+2}]^T$$

and

$$Y_i = \begin{bmatrix} \lambda_i & 1-\lambda_i-\mu_i & \mu_i & \\ & 1-\alpha_i & \alpha_i & \\ & \beta_i & 1-\beta_i & \\ & \lambda_{i+1} & 1-\lambda_{i+1}-\mu_{i+1} & \mu_{i+1} \end{bmatrix} \quad (3.7)$$

Then the transformation (3.6) can also be represented in matrix notation as

$$X_i = Y_i.Z_i \quad (3.8)$$

The transformation to rational Bernstein-Bezier form is very convenient for computational purposes.

3.4 Shape Control

The parameters defined in equation(3.1) can be used to control the local or global shape of the curve. These shape control properties of the rational B-spline are analysed as follows:

1. *Point Tension.* Consider $v_i \to \infty$. Then
   $lim\ W_{i-1} = lim\ V_i = lim\ F_i = P_i$.
   Thus the curve is pulled towards P_i and in the limit a tangent discontinuity is introduced at P_i.

2. *Interval Tension.* Consider v_i, $v_{i+1} \to \infty$. Then

   $lim\ W_{i-1} = lim\ V_i = lim\ F_i = P_i$

   and

   $lim\ W_i = lim\ V_{i+1} = lim\ F_{i+1} = P_{i+1}$

   Thus the curve is pulled towards the straight line segment:

   $P_i(1-\theta) + P_{i+1}\theta$

   and in the limit a tangent discontinuity is introduced at P_i, P_{i+1}.

3. *Global Tension.* Consider $v_i \to \infty$, $\forall\ i$, following the above tension results, one can easily see that the curve is pulled towards the control polygon $\{P_1, P_2, \ldots\ldots, P_{n-1}\}$

3.4.1 Examples

The tension behaviors of the rational cubic spline (ANURBS) are illustrated by the following simple examples for the data set in R^2. It should be noted that unless otherwise stated we shall assume $v_i = 1, \forall\ i$. The point tension behavior is shown in Figure 3.1(a), as v_2 is increased the resulting curve is pulled towards P_2. When the point tension is increased at two consecutive points P_2 and P_3 the resulting curve is pulled towards the straight line segment P_2P_3, as shown in Figure 3.1(b). The global tension behavior is shown in Figure 3.2 where all shape parameters are progressively increased with values 1, 5 and 50. The effect of the high tension parameters is clearly seen in that the resulting spline curve Figure 3.2(c) approaches the control polygon. Figure 3.3(b) displays the point tension result to ANURBS curve of Figure 3.3(a) at the top most point.

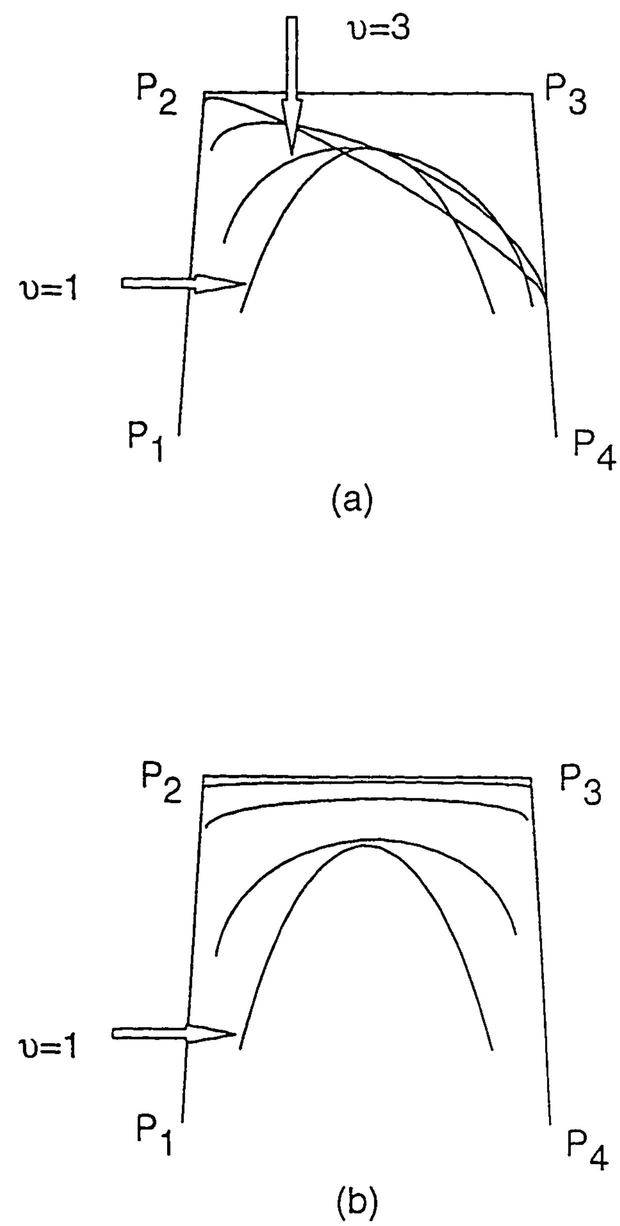

Figure 3.1: Point tension behavior

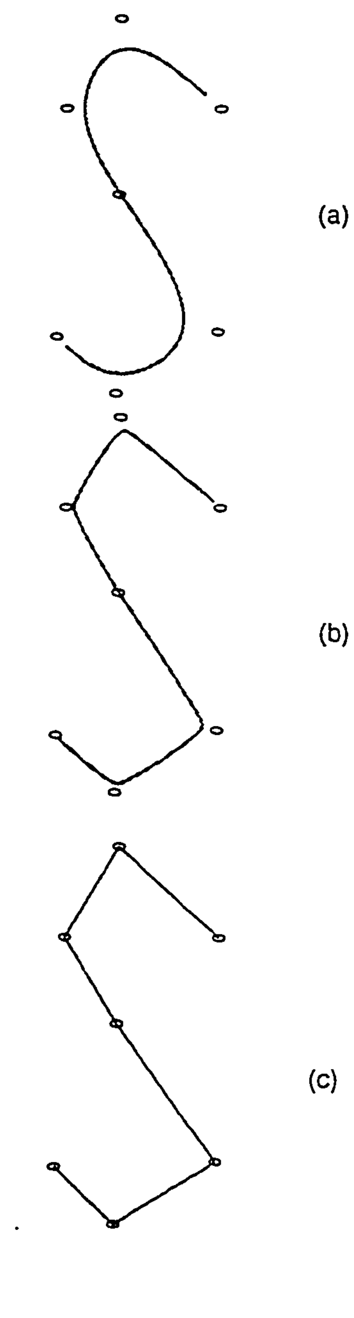

Figure 3.2: Curves, with global tension

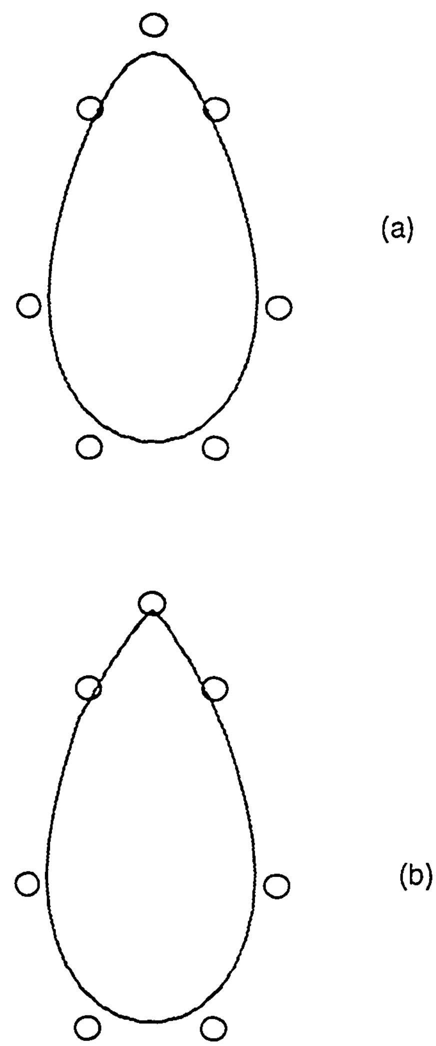

Figure 3.3: Curves, with point tension

3.5 Interpolatory B-Spline with Point Tension

The process of obtaining the interpolatory rational cubic B-spline with point tension is accomplished by furthering the work done in [18]. The derivation procedure is shown below:

A convenient method for computing the curve representation of [18] is given by :

$$\sum_{j=-1}^{n+1} P_j B_j(t_i) = F_i \tag{3.9}$$

where $B_j(t)$'s are B-spline blending functions. At $t = t_i$ all $B_i(t_i)$'s are zero except $B_{i-1}(t_i)$, $B_i(t_i)$, and $B_{i+1}(t_i)$. From equation(3.6) we have:

$$P_{i-1}\lambda_i + P_i(1 - \lambda_i - \mu_i) + P_{i+1}\mu_i = F_i \tag{3.10}$$

The above set of equations for F_i, $i = 0,..,n$ (given set of data points) and new control points P_i's (to be determined) can be written in the matrix form as follows:

$$X.P = F \tag{3.11}$$

Where the values of matrices X, P and F are as shown in Figure 3.4.

As such the above system is underdefined and for a unique solution we need to specify two further conditions at the start and the end of the curve. We shall make the two end control points coincident, although it is not the only end condition available. The above system of equations is tridiagonal-only the diagonal elements and the two neighbors are nonzero. By exploiting the structure of the tridiagonal matrix we can solve more efficiently and bypass the standard elimination techniques.

$$X = \begin{bmatrix} 1-\lambda_0-\mu_0 & \mu_0 & & & & \\ \lambda_1 & 1-\lambda_1-\mu_1 & \mu_1 & & & \\ & \lambda_2 & 1-\lambda_2-\mu_2 & \mu_2 & & \\ & & \cdots & \cdots & \cdots & \\ & & & \lambda_{n-1} & 1-\lambda_{n-1}-\mu_{n-1} & \mu_{n-1} \\ & & & & \lambda_n & 1-\lambda_n-\mu_n \end{bmatrix}$$

$$P = \begin{bmatrix} P_0 \\ P_1 \\ P_2 \\ P_3 \\ \vdots \\ P_n \end{bmatrix} \qquad F = \begin{bmatrix} F_0 \\ F_1 \\ F_2 \\ \vdots \\ F_n \end{bmatrix}$$

Figure 3.4: Values of matrices X, P and F

From equation(3.11), we get

$$P = X^{-1}F \tag{3.12}$$

That is the control points of the curve, which passes through the given data points F's are given by the above equation. When these values are substituted in the equation(3.4), we get the required C^2 interpolatory B-spline curve with point tension.

3.5.1 Examples

The shape behaviors of the interpolatory rational spline with point tension are illustrated by the following simple examples for the data set in R^2. The global tension behavior is shown in Figure 3.5 where all shape parameters are progressively increased with values 1, 5, 50. The effect of the high point tension is clearly seen in that the resulting spline curve Figure 3.5(c) approaches the control polygon. Figure 3.6(b) displays the point tension result to the curve of Figure 3.5(a) at the top most point.

3.6 Surfaces

The results of section(3.3) can be extended to tensor product rational bicubic B-spline surfaces, that is surfaces of the form

$$p(\tilde{t}, t) = \sum_{k=-1}^{m+1} \sum_{l=-1}^{n+1} P_{k,l} \tilde{B}_k(\tilde{t}, t) B_l(t, \tilde{t}) \tag{3.13}$$

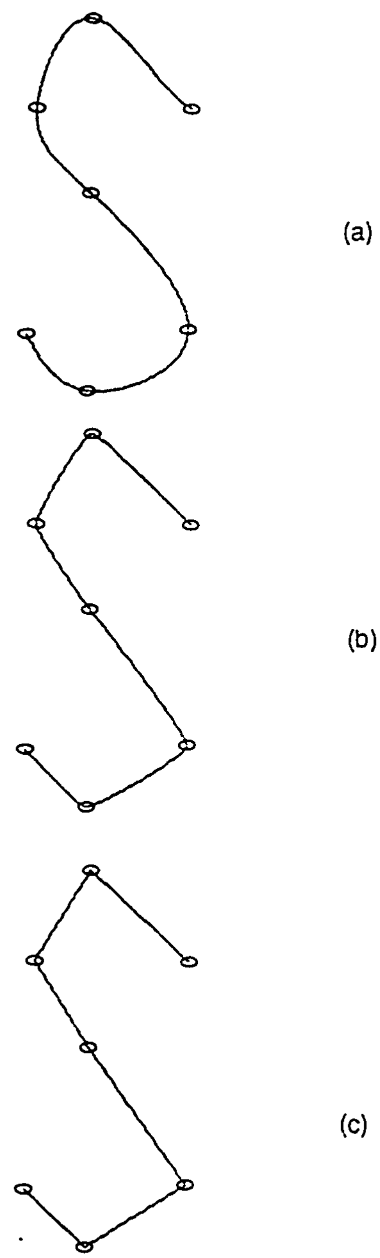

Figure 3.5: Interpolatory curves, with global tension

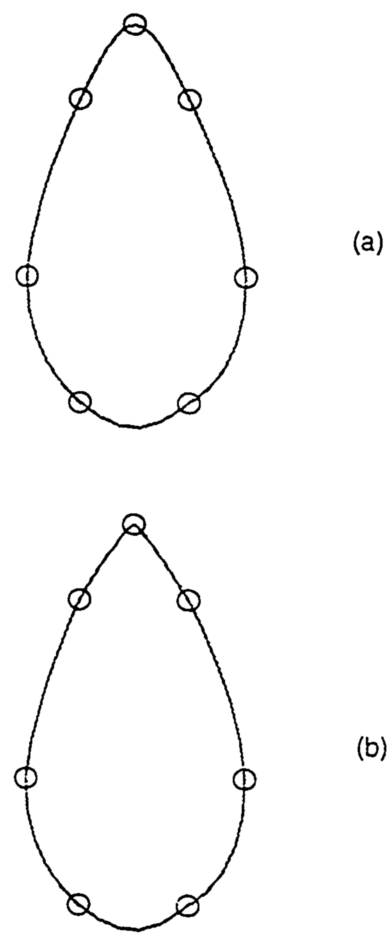

Figure 3.6: Interpolatory curves, with local tension

$t_0 \leq t \leq t_n$, $\tilde{t}_0 \leq \tilde{t} \leq \tilde{t}_n$ with $B_l(t)$ as constructed in section(3.3) and analogously the $\tilde{B}_k(\tilde{t})$ a set of rational cubic B-splines corresponding to a set of knots $\tilde{t}_k$. $k = -3, \ldots, m+3$ (m ≥ 0), with shape parameters $\tilde{v}_k$, $k = 3, \ldots, m+3$
If the representation of a rational spline patch $p(\tilde{t}, t)$, $\tilde{t}_i \leq \tilde{t} \leq \tilde{t}_{i+1}$, $t_j \leq t \leq t_{j+1}$ is required as a rational bicubic Bernstein-Bezier patch, then it can be expressed as:

$$p_{i,j}(\tilde{t}, t) = \sum_{k=0}^{3}\sum_{l=0}^{3} X_{k,l}^{i,j}(\tilde{t}, t) R_k(\tilde{\theta}; \tilde{r}_i(t)) R_l(\theta; r_j(\tilde{t})). \quad (3.14)$$

Here $\tilde{r}_i(t)$ and $r_j(t)$ are variable cubic B-spline tensions defined as:

$$\tilde{r}_i(t) = \sum_j \tilde{v}_{i,j} N_j(t). \quad (3.15)$$
$$r_j(\tilde{t}) = \sum_i v_{i,j} N_i(\tilde{t})$$

where $N_i(t)$'s are cubic B-splines. These can be computed as a special case of the rational cubic splines of section(3.3).
The Bernstein-Bezier points $X_{k,l}^{i,j}$ can be computed from the rational B-spline vertices $P_{i,j}$ as

$$X_{i,j} = Y_i . Z_{i,j} . Y_j^T \quad (3.16)$$

where

$$X_{i,j} = \begin{bmatrix} X_{0,0}^{i,j} & X_{0,1}^{i,j} & \ldots & X_{0,3}^{i,j} \\ X_{1,0}^{i,j} & \ldots & \ldots & \ldots \\ \ldots & \ldots & \ldots & \ldots \\ X_{3,0}^{i,j} & \ldots & \ldots & X_{3,3}^{i,j} \end{bmatrix}$$

$$Z_{i,j} = \begin{bmatrix} P_{i-1,j-1} & P_{i-1,j} & \dots & P_{i-1,j+2} \\ P_{i,j-1} & \dots & \dots & \dots \\ \dots & \dots & \dots & \dots \\ P_{i+2,j-1} & \dots & & P_{i+2,j+2} \end{bmatrix}$$

and the matrix Y_i is given as in equation(3.7) with a corresponding expression for $\tilde{Y}_i$.

3.6.1 Remarks

There is a drawback with this ANURBS surfaces in that any of the shape parameters influences entire corresponding row or column of the surface. The drawback of not having local control for ANURBS can be removed: A surface method, using the rational cubic splines of [14] , may be utilized to control the shape of the surface both locally and globally. This is a simple bivariate B-spline product method which results in a C^2 freeform surface as well as provides shape control. This method is similar to a tensor product method but actually it is not. C^2 variable tensions are introduced in the B-splines which distinguish this surface method from the tensor product method and help in producing a C^2 surface which has tension control both locally and globally. The surfaces of this section follow the method of [14] to alleviate the drawback of ANURBS surface. Hence generating surfaces which are C^2 and have both local and global control.

3.7 Interpolatory Surfaces

Expanding equation(3.16) we get the points through which the freeform rational B-spline surface passes, for given control points say P's. Here in our case we need to find P's (the new control points) given the data points F's, through which the interpolatory rational B-spline surface should pass. Let us denote it by F:

$$\begin{aligned} F_{i,j} = X = \tilde{\lambda}_i[P_{i-1,j-1}\lambda_j + P_{i-1,j}(1-\lambda_j-\mu_j) + P_{i-1,j+1}\mu_j] + \\ (1-\tilde{\lambda}_i-\tilde{\mu}_i)[P_{i,j-1}\lambda_j + P_{i,j}(1-\lambda_j-\mu_j) + P_{i,j+1}\mu_j] + \\ \tilde{\mu}_i[P_{i+1,j-1}\lambda_j + P_{i+1,j}(1-\lambda_j-\mu_j) + P_{i+1,j+1}\mu_j] \end{aligned} \quad (3.17)$$

For $i = 1,\ldots,n$ and $j = 1,\ldots,m$;

We can observe from the above that the sum of the coefficients of P's equal to unity. which means that the resulting interpolatory surface satisfies the *convex hull property*. Let

$$A_{i,j} = P_{i,j-1}\lambda_j + P_{i,j}(1-\lambda_j-\mu_j) + P_{i,j+1}\mu_j \quad (3.18)$$

Equation(3.17) can be expressed as :

$$F = T.A \quad (3.19)$$

where F. T. and A are as given below:

$$T = \begin{bmatrix} 1-\hat{\lambda}_1-\hat{\mu}_1 & \hat{\mu}_1 & & & & \\ \hat{\lambda}_2 & 1-\hat{\lambda}_2-\hat{\mu}_2 & \hat{\mu}_2 & & & \\ & \hat{\lambda}_3 & 1-\hat{\lambda}_3-\hat{\mu}_3 & \hat{\mu}_3 & & \\ & & \hat{\lambda}_4 & 1-\hat{\lambda}_4-\hat{\mu}_4 & \hat{\mu}_4 & \\ & & & & & \\ & & & & \hat{\lambda}_m & 1-\hat{\lambda}_m-\hat{\mu}_m \end{bmatrix}$$

$$A = \begin{bmatrix} A_{1,1} \\ A_{2,1} \\ . \\ . \\ A_{m-1,1} \\ A_{m,1} \end{bmatrix} \quad \text{and} \quad F = \begin{bmatrix} F_{1,1} \\ F_{2,1} \\ \\ . \\ F_{m-1,1} \\ F_{m,1} \end{bmatrix}$$

Since T is invertible. from equation(3.19). we get

$$A = T^{-1}.F \tag{3.20}$$

Moreover A can be expressed as:

$$A = D.P \tag{3.21}$$

The values of A. P. and D are as given below:

$$D = \begin{bmatrix} 1-\lambda_1-\mu_1 & \mu_1 & & & & & \\ \lambda_2 & 1-\lambda_2-\mu_2 & \mu_2 & & & & \\ & \lambda_3 & 1-\lambda_3-\mu_3 & \mu_3 & & & \\ & & \lambda_4 & 1-\lambda_4-\mu_4 & \mu_4 & & \\ & & & & & & \\ & & & & & \lambda_n & 1-\lambda_n-\mu_n \end{bmatrix}$$

$$A = \begin{bmatrix} A_{i,1} \\ A_{i,2} \\ . \\ . \\ A_{i,n-1} \\ A_{i,n} \end{bmatrix} \quad \text{and} \quad P = \begin{bmatrix} P_{i,1} \\ P_{i,2} \\ \\ . \\ P_{i,n-1} \\ P_{i,n} \end{bmatrix}$$

The process of calculating the new control points P's is carried out in two stages. first the entire matrix A is calculated. Then the new control points P's can be calculated as

$$P = D^{-1}.A \tag{3.22}$$

which when substituted in equation(3.14), gives the required interpolatory surface with point tension which can be controlled both locally and globally.

3.7.1 Examples

Consider a data set of a cup in R^3. The figures show the effect of increase in tensions, both locally and globally. The surface in Figure 3.7 corresponds to global values $v = \tilde{v} = 3$ (the bicubic spline surface). Figure 3.8 shows the global tension effects in both directions ($v = \tilde{v} = 50$). Figure 3.9 is an example of the effect of increasing the v shape parameters in both directions on a point at the top of the cup, and hence creating a corner. The surface of Figure 3.10(a) is a bicubic spline surface. the surfaces in Figures 3.10(b) and 3.11(a) are due to high global tension values in $\tilde{t}$ and t directions respectively; the surface of Figure 3.11(b) is obtained when all tension parameters. in both directions. are assumed equal to 50. Figure 3.12 shows the point tension effect at the top most point.

3.8 Concluding Remarks

An analysis of a C^2 interpolatory rational cubic spline is developed with a view to its application in CAD/CAM and Computer Graphics. It provides local as well as global shape controls. In particular, it has been found that only one shape parameter per point is enough when local or global shape control, in any portion of the figure, is required. The rational spline method can be applied to tensor product surfaces but unfortunately, in the context of interactive surface design, this tensor product surface is not that useful because any of the shape parameters controls an entire corresponding strip of the surface. The NURBS. are popular regarding local shape control but the user has to be careful because of certain limitations of the nature

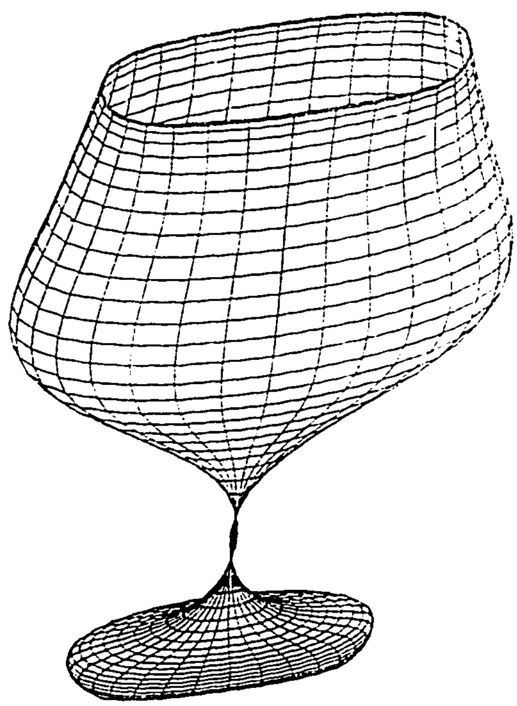

Figure 3.7: The bicubic spline surface

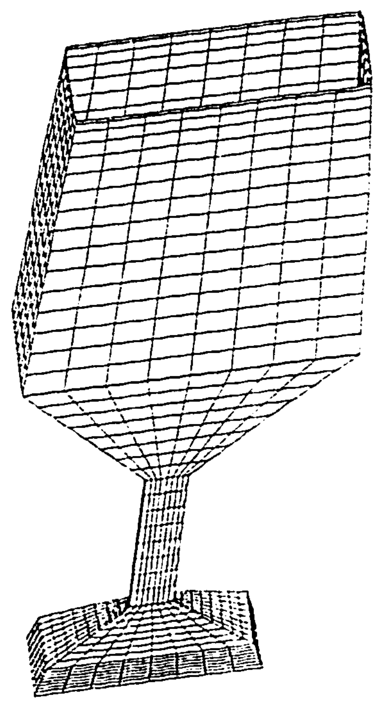

Figure 3.8: Global tension effect

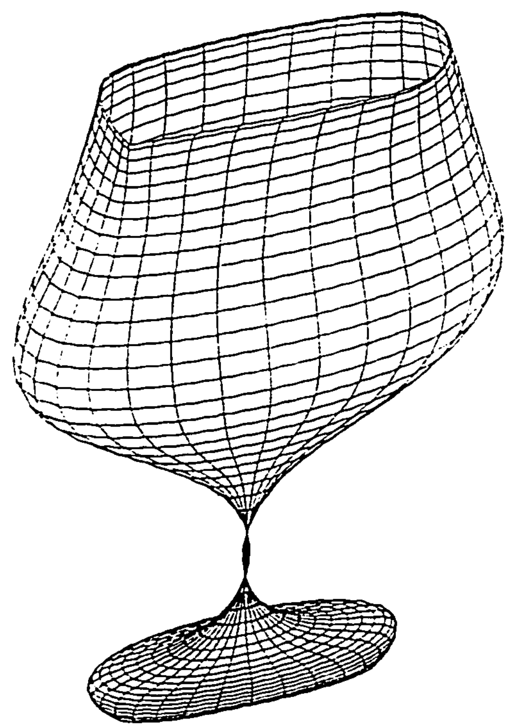

Figure 3.9: Point tension effect

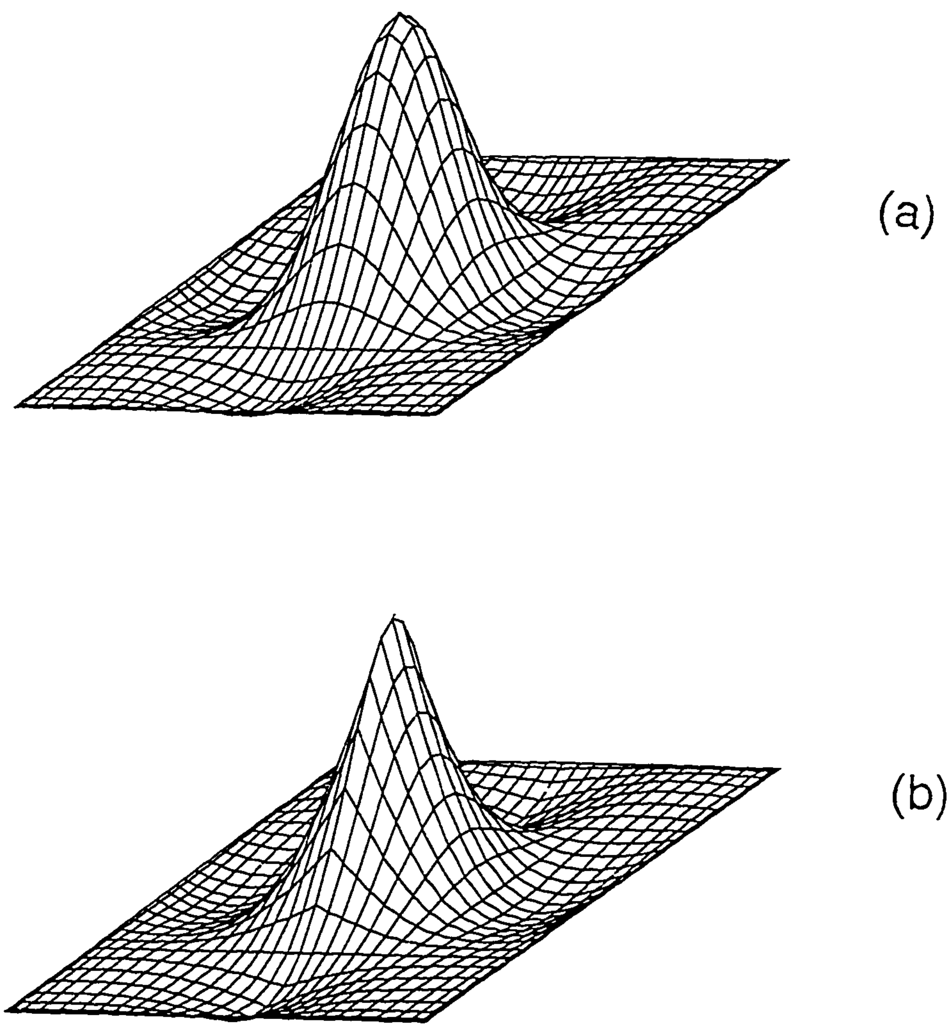

Figure 3.10: Interpolatory surfaces

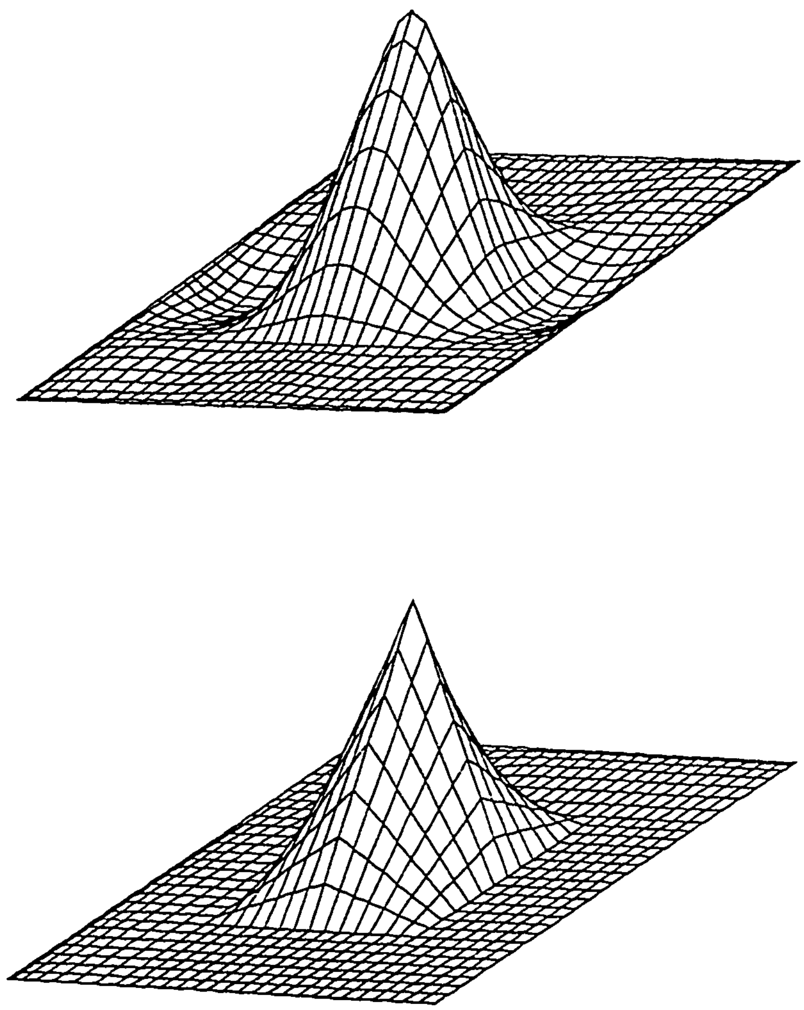

(a)

(b)

Figure 3.11: Interpolatory surfaces

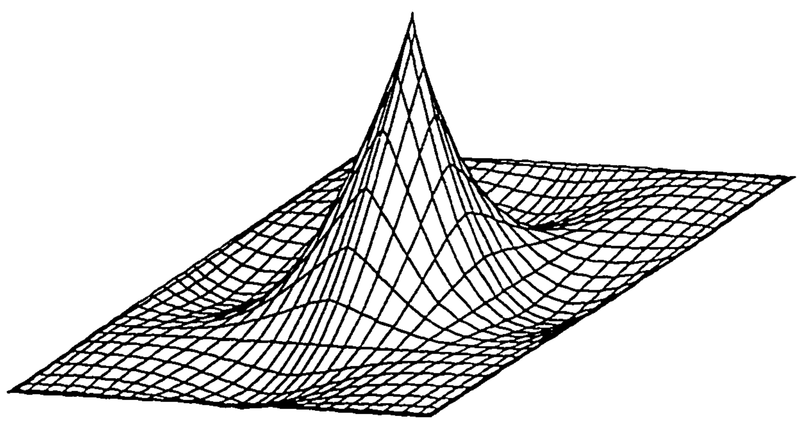

Figure 3.12: Interpolatory surfaces

of the shape parameters in the construction of the NURBS. Thus some useful and sufficiently smooth method is required so that one may play with the shape of the surfaces freely. The method in the previous section of this chapter provides such features.

Chapter 4

POINT AND INTERVAL TENSION SPLINES

4.1 Introduction

This chapter describes a parametric C^2 rational spline representation [19] which has interval and point tension weights which can be used to control the shape of the curve. The spline can be considered as an alternative to the cubic ν-spline and β-spline formulations of [12] and [6]. These splines provide shape control parameters through the use of geometric GC^2 continuity constraints and hence are C^2 with respect to a reparameterization. The rational spline also provides a C^2 alternative to the C^1 weighted ν-spline of Foley[1], since the interval and point tension weights have a remarkably similarly influence on the curve to those of the weighted ν-spline.

The rational spline. discussed here is a generalization of the interval tension method introduced in [2]. However, the appropriate generalization of this interval tension method is not immediately clear. The use of a general rational form gives an over abundance of conflicting parameters which can lead to poorly parameterized curves. The solution adopted here is to restrict the class of rational cubic representations to those having quadratic denominators. This leads to representations having sensible parameterizations with well defined and well behaved interval and point tension weights. The use of this restricted class of rational splines has the added advantage that conic segments could easily be accommodated within the representation.

Given the volume of literature on rational splines in CAD, the reader might be dubious as to the merit of introducing yet another rational spline representation. However, we believe that the introduction of point and interval weights gives a powerful tool for manipulating the shape of the curve within one simple representation and hence will be useful in CAD applications. The spline can be represented as a NURB through the use of multiple knots, although we prefer the direct use of the rational Bernstein-Bezier basis in the development of the theory. In section(4.2), the basis rational cubic form is described. Then, in section(4.3), the local support basis form is described. Section(4.4) describes B-spline like interpolatory rational spline with point and interval tension. Section(4.5) and section(4.6) describe freeform and interpolatory surfaces respectively.

4.2 The Rational Cubic Form

Let $F_i \in R^m$, $i \in Z$, be values given at the distinct knots $t_i \in R$, $i \in Z$. A parametric C^1 piecewise rational cubic Hermite function $p : R \to R^m$ is defined by

$$p_{[t_i,t_{i+1}]}(t) = N(\theta)/D(\theta). \tag{4.1}$$

where

$N(\theta) = (1-\theta)^3\alpha_i F_i + \theta(1-\theta)^2(\alpha_i + \gamma_i)V_i + \theta^2(1-\theta)(\beta_i + \gamma_i)W_i + \theta^3\beta_i F_{i+1}$.

$D(\theta) = (1-\theta)^2\alpha_i + \gamma_i\theta(1-\theta) + \theta^2\beta_i$.

with

$$V_i = F_i + \frac{\alpha_i}{\alpha_i + \gamma_i}h_i D_i, \tag{4.2}$$
$$W_i = F_{i+1} - \frac{\beta_i}{\beta_i + \gamma_i}h_i D_{i+1}$$

For simplicity, we assume positive weights

$$\lambda_i > 0, \; \mu_i > 0 \text{ and } \gamma_i \geq 0, \quad i \in Z \tag{4.3}$$

and have made use of a rational Bernstein-Bezier representation, where the control points $\{F_i, V_i, W_i, F_{i+1}\}$ are determined by imposing the the Hermite interpolation conditions:

$$p(t_i) = F_i$$

and $p^{(1)}(t_i) = D_i,\ i \in Z$.

Since the denominator is positive, it follows from Bernstein-Bezier theory that the curve segment $p_{[t_i,t_{i+1}]}$ lies in the convex hull of the control points $\{F_i, V_i, W_i, F_{i+1}\}$ and is variation diminishing with respect to the control polygon joining these points.

For the practical implementation we will write

$$\alpha_i = 1/\lambda_i \text{ and } \beta_i = 1/\mu_i \tag{4.4}$$

This leads to a consistent behavior with respect to increasing weights and avoids numerical problems associated with evaluation at $\theta = 0$ and $\theta = 1$ in the (removable) singular cases $\alpha_i = 0$ and $\beta_i = 0$. We now have

$$\begin{aligned} V_i &= F_i + \frac{1}{\lambda_i\gamma_i + 1} h_i D_i, \\ W_i &= F_{i+1} - \frac{1}{\mu_i\gamma_i + 1} h_i D_{i+1} \end{aligned} \tag{4.5}$$

The following *tension* properties of the rational Hermite form are now immediately apparent from equations(4.1),(4.4) and (4.5), see Figure 4.1

1. **Point tension**

   $\lim_{\lambda_i \to \infty} V_i = F_i$ and

   $\lim_{\lambda_i \to \infty} p_{[t_i,t_{i+1}]}(t) = N(\theta)/D(\theta)$,

   where

   $N(\theta) = (1-\theta)^2\gamma_i F_i + \theta(1-\theta)(\beta_i + \gamma_i)W_i + \theta^2\beta_i F_{i+1}$,

   $D(\theta) = (1-\theta)\gamma_i + \theta\beta_i$,

   $\lim_{\mu_i \to \infty} W_i = F_{i+1}$ and

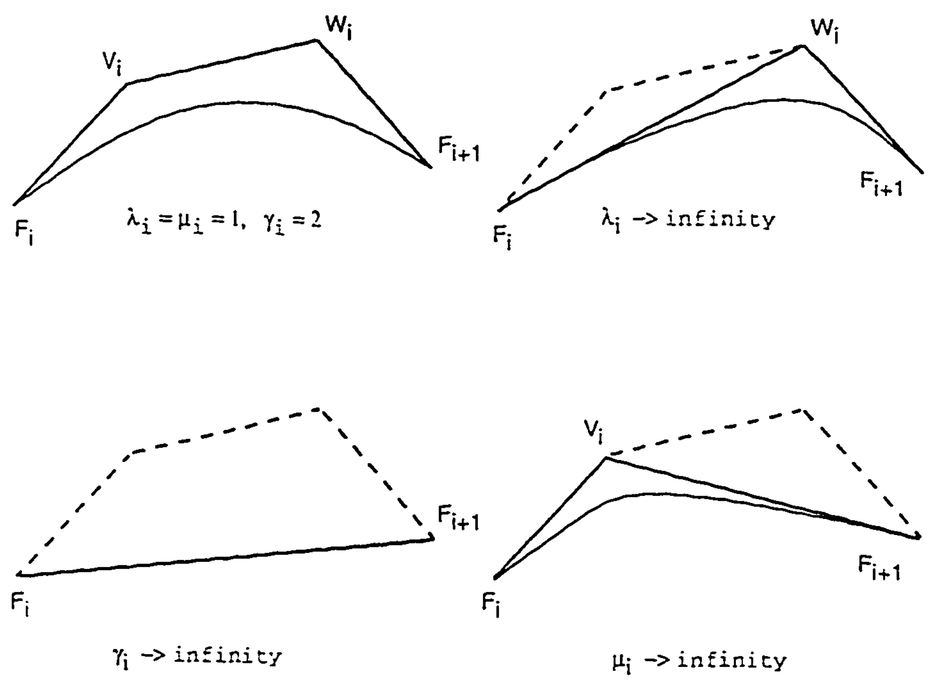

Figure 4.1: Tension properties of the rational cubic Hermite

$\lim_{\mu_i \to \infty} p_{[t_i,t_{i+1}]}(t) = N(\theta)/D(\theta)$,

where

$N(\theta) = (1-\theta)^2\alpha_i F_i + \theta(1-\theta)(\alpha_i + \gamma_i)V_i + \theta^2\gamma_i F_{i+1}$.

$D(\theta) = (1-\theta)\alpha_i + \theta\gamma_i$.

2. **Interval tension**

   $\lim_{\gamma_i \to \infty} V_i = F_i$, $\lim_{\gamma_i \to \infty} W_i = F_{i+1}$. and

   $\lim_{\gamma_i \to \infty} p_{[t_i,t_{i+1}]}(t) = (1-\theta)F_i + \theta F_{i+1}$

   For more detail regarding shape analysis the reader is referred to [19].

4.3 The Local Support Basis

We now describe a local support basis representation for the space of C^2 rational cubic splines on the knot partition ($t_i \in R$. $i \in Z$). Thus assume that there exists a local support basis ($B_j(t)$)$_{j \in Z}$, where

1. $B_j(t) = 0$. $t \notin (t_{j-2}, t_{j+2})$. (local support)

2. $\sum_{j \in Z} B_j(t) = 1$. (partition of unity: normalization)

Then given control points $\{P_j \in R^m, \ j \in Z\}$. we consider the parametric curve representation

$$p(t) = \sum_{j \in Z} P_j B_j(t) \qquad (4.6)$$

Following the approach of Boehm [13], the curve is represented in the rational Bernstein-Bezier form, as in equation(4.1), with control points $\{F_i, V_i, W_i, F_{i+1}\}_{i\in Z}$. The existence of the transformation to rational Bernstein-Bezier form will in fact, demonstrate the existence of the local support basis. The transformation also provides a convenient tool for computing and analysing the local support basis representation.

Imposing the constraint

$$p^{(1)}(t_i^+) = p^{(1)}(t_i^-) \tag{4.7}$$

on the rational Bernstein-Bezier form gives

$$F_i = (1-\delta_i)W_{i-1} + \delta_i V_i \tag{4.8}$$

where

$$\delta_i = \frac{h_{i-1}(\gamma_i\lambda_i+1)}{h_{i-1}(\gamma_i\lambda_i+1)+h_i(\gamma_{i-1}\mu_{i-1}+1)}$$

Also, imposing the constraint

$$p^{(2)}(t_i^+) = p^{(2)}(t_i^-) \tag{4.9}$$

and some further processing gives the values of V_i's and W_i's

$$V_i = [(1-\tau_i)/\Delta_i]P_i - [\sigma_i/\Delta_i]P_{i+1} \tag{4.10}$$

$$W_i = -[\tau_i/\Delta_i]P_i + [(1-\sigma_i)/\Delta_i]P_{i+1}$$

where

$$\Delta_i = 1 - \sigma_i - \tau_i \tag{4.11}$$

τ_i and σ_i are the values as given in [19]. Equations(4.10) and (4.11) define the transformation from the control points $\{P_i\}_{i\in Z}$ to those of the piecewise defined Bernstein-Bezier representation. The existence of this transformation implies the existence of the local support basis.

4.3.1 Tension Properties

We know consider the tension properties of the local support basis representation:

Point Tension: Consider $\lambda_i \to \infty$ and let $\hat{V}_i$ be defined by equation(4.10) with weights $\hat{\sigma}_i = \lim \sigma_i$ and $\hat{\tau}_i = \lim \tau_i$. Then

$$\lim F_i = \lim V_i = \hat{V}_i \text{ and } \lim W_{i-1} = P_i. \tag{4.12}$$

Thus the curve is pulled towards a point $\hat{V}_i$ on the line segment joining P_i and P_{i+1} and, in the limit, is C^1 at $\hat{V}_i$.

Interval Tension: Consider $\gamma_i \to \infty$. In this case

$\lim F_i = \lim V_i = \hat{V}_i$, $\lim F_{i+1} = \lim W_i = \hat{W}_i$,

$\lim W_{i-1} = P_i$, $\lim V_{i+1} = P_{i+1}$.

As proved in [19]. The curve is pulled onto a straight line segment joining the points $\hat{V}_i$ and $\hat{W}_i$ between P_i and P_{i+1}.

4.3.2 Examples

The behavior described above is confirmed by the examples curves of Figures 4.2 and 4.3.

4.4 Interpolatory Spline with Interval and Point Tension

The process of obtaining the interpolatory rational cubic B-spline with interval shape control is accomplished through

$$p(t) = \sum_{j \in Z} P_j B_j(t) \tag{4.13}$$

From equation(4.8) F_i's, $i = 0, \ldots, n$ can be written as

$$F_i = \kappa_i P_{i-1} + \rho_i P_i + \phi_i P_{i+1} \tag{4.14}$$

where

$$\kappa_i = [1 - \delta_i](\tau_{i-1}/\Delta_{i-1})$$

$$\rho_i = [1 - \delta_i][(1 - \sigma_{i-1})/\Delta_{i-1}] + \delta_i[(1 - \tau_i)/\Delta_i]$$

$$\phi_i = \delta_i(\sigma_i/\Delta_i)$$

Let

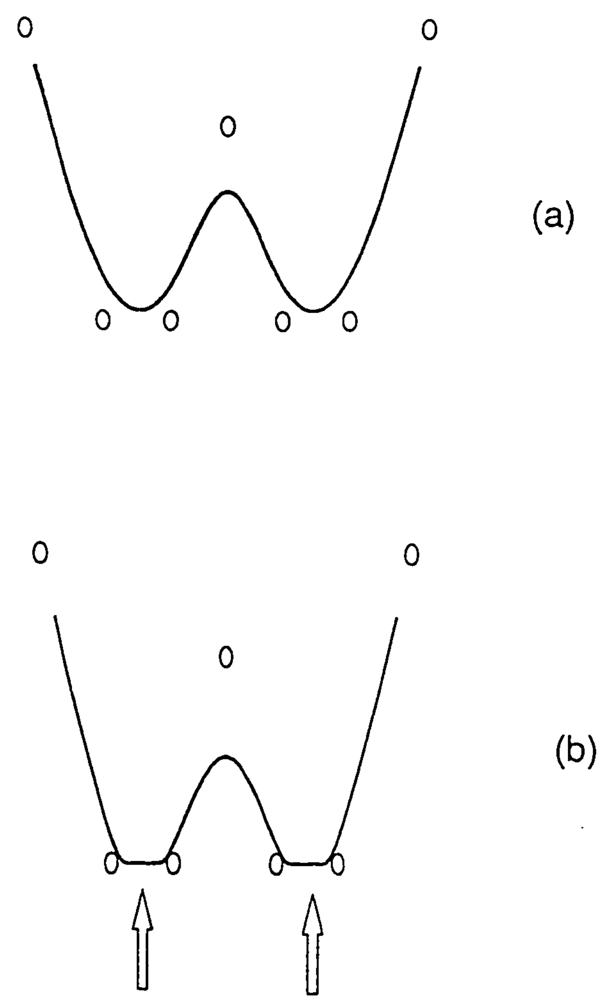

Figure 4.2: Curves with point and interval tension

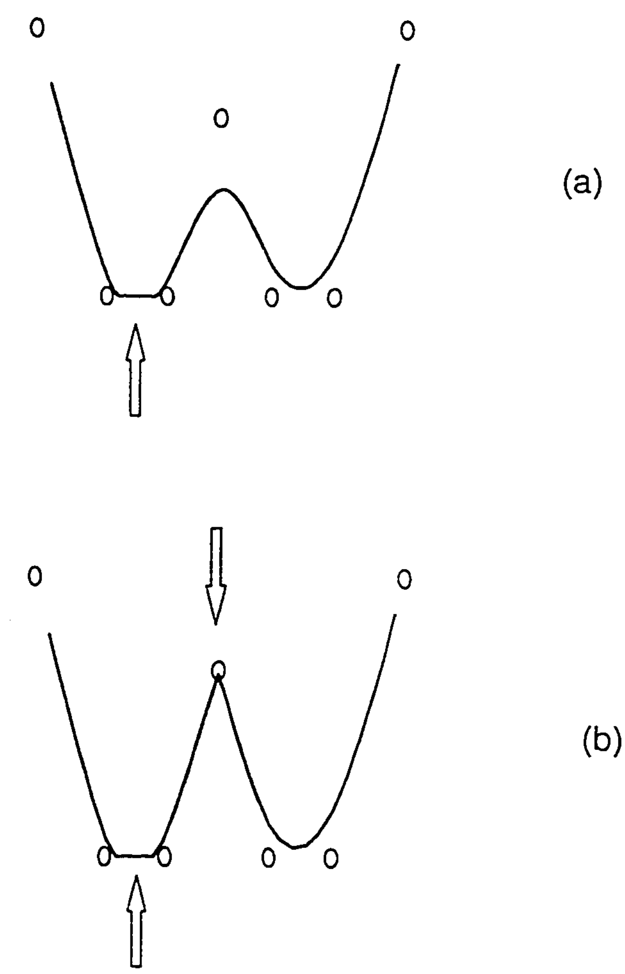

Figure 4.3: Curves with point and interval tension

$$X_i=[F_i\ V_i\ W_i\ F_{i+1}]^T,\ Z_i=[P_{i-1}\,P_i\,P_{i+1}\,P_{i+2}]^T$$

and

$$Y_i = \begin{bmatrix} \kappa_i & \rho_i & o_i & \\ & tv1_i & tv2_i & \\ & tw1_i & tw2_i & \\ & \kappa_{i+1} & \rho_{i+1} & o_{i+1} \end{bmatrix} \quad (4.15)$$

Where

$$tv1_i = [(1-\tau_i)/\Delta_i]$$
$$tv2_i = -[(\sigma_i/\Delta_i)]$$
$$tw1_i = -[(\tau_i/\Delta_i)]$$

and

$$tw2_i = [(1-\sigma_i)/\Delta_i]$$

Then the transformation (4.14) can also be represented in matrix notation as

$$X = Y.Z \quad (4.16)$$

Equation(4.14), for $i = 0,\ldots,n$ can be written in matrix form as:

$$F = T.P \quad (4.17)$$

The given set of data points F's, through which the resulting curve must pass, and the new control points P's can be written as in equation(4.17). The values of F, P and T are as shown below. As such the above system is underdefined and for a unique solution we need to specify two further conditions, one at the start and one at the end of the curve. We shall repeat the two end control points, although it is not the only end condition available. The above system of equations is tridiagonal-only the diagonal elements and the two neighbors are nonzero. By exploiting the structure of the tridiagonal matrix we can solve the resulting system of equations more efficiently and bypass the standard elimination techniques.

$$\mathrm{T} = \begin{bmatrix} \rho_1 & \sigma_1 & & & & \\ \kappa_2 & \rho_2 & \sigma_2 & & & \\ & \kappa_3 & \rho_3 & \sigma_3 & & \\ & & \kappa_4 & \rho_4 & \sigma_4 & \\ & & & & & \\ & & & & \kappa_n & \rho_n \end{bmatrix}$$

$$\mathrm{P} = \begin{bmatrix} P_0 \\ P_1 \\ P_2 \\ . \\ . \\ . \\ P_{n-1} \\ P_n \end{bmatrix} \quad \mathrm{F} = \begin{bmatrix} F_0 \\ F_1 \\ F_2 \\ . \\ . \\ . \\ F_{n-1} \\ F_n \end{bmatrix}$$

From equation(4.17), we get

$$P = T^{-1}.F \tag{4.18}$$

That is the control vertices of the curve which passes through the given data points F's are given by the P's as in equation(4.18). When these values of P's are substituted in equation(4.13), we get the required C^2 interpolatory B-spline curve with point and interval tension.

4.4.1 Examples

The shape behavior of the interpolatory rational spline with point and interval tension is illustrated by following simple examples for the data set in R^2. The behavior described above is confirmed by the example curves of Figure 4.4.

4.5 Surfaces

The results of section(4.3) can be extended for tensor product rational bicubic B-spline surfaces. That is surfaces of the form

$$p(\tilde{t}, t) = \sum_{k=i-1}^{i+2} \sum_{l=j-1}^{j+2} P_{k,l} \tilde{B}_k(\tilde{t}, t) B_l(t, \tilde{t}) \tag{4.19}$$

with $B_l(t)$ as constructed in section(4.3) and analogously the $\tilde{B}_k(\tilde{t})$ a set of rational cubic B-splines corresponding to a set of knots $\tilde{t}$, $k = -3, \ldots, m+3$ (m ≥ 0), with corresponding shape parameters.

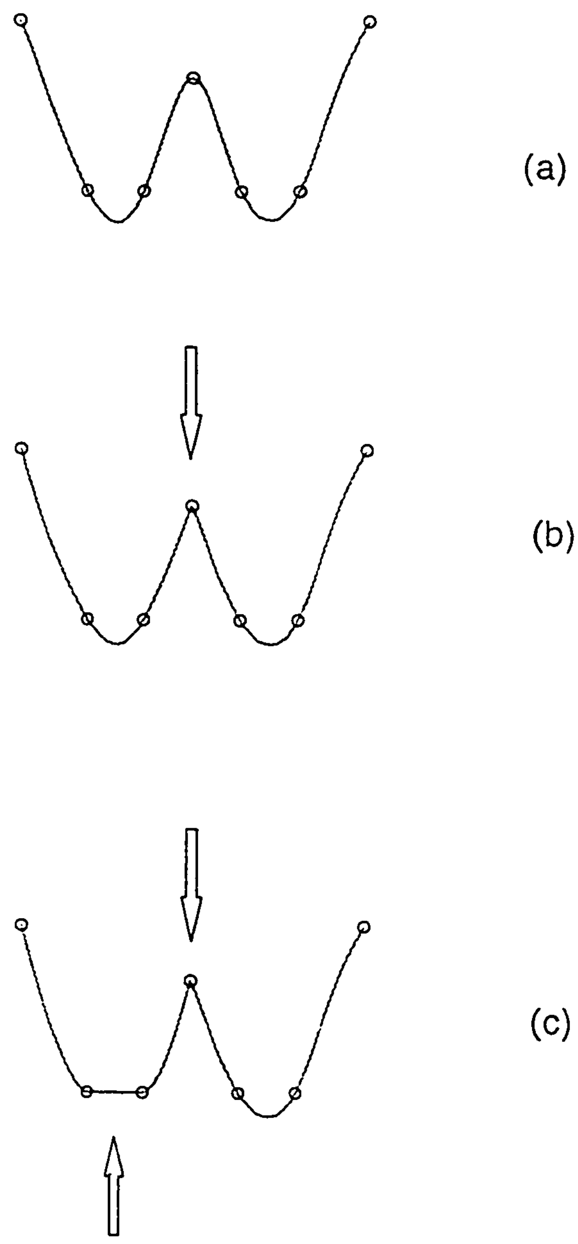

Figure 4.4: Interpolatory curves with point and interval tension

If the representation of a rational spline patch $p(\tilde{t},t)$, $\tilde{t}_i \leq \tilde{t} \leq \tilde{t}_{i+1}$, $t_j \leq t \leq t_{j+1}$ is required as a rational bicubic Bernstein-Bezier patch, then it can be expressed as:

$$p(\tilde{t},t) = \sum_{k=0}^{3}\sum_{l=0}^{3} X_{k,l}^{i,j}(\tilde{t},t) R_k(\tilde{\theta}; \tilde{r}_i(t)) R_l(\theta; r_j(\tilde{t})), \tag{4.20}$$

the Bernstein-Bezier points $X_{k,l}^{i,j}$ can be computed from the rational B-spline vertices $P_{i,j}$ as

$$X_{i,j} = \tilde{Y}_i \,.Z_{i,j}\,.Y_j^T \tag{4.21}$$

where

$$X_{i,j} = \begin{bmatrix} X_{0,0}^{i,j} & X_{0,1}^{i,j} & \cdots & X_{0,3}^{i,j} \\ X_{1,0}^{i,j} & \cdots & \cdots & \cdots \\ \cdots & \cdots & \cdots & \cdots \\ X_{3,0}^{i,j} & \cdots & \cdots & X_{3,3}^{i,j} \end{bmatrix}$$

$$Z_{i,j} = \begin{bmatrix} P_{i-1,j-1} & P_{i-1,j} & \cdots & P_{i-1,j+2} \\ P_{i,j-1} & \cdots & \cdots & \cdots \\ \cdots & \cdots & \cdots & \cdots \\ P_{i+2,j-1} & \cdots & & P_{i+2,j+2} \end{bmatrix}$$

and the matrix Y_i is given as in equation(4.15) with a corresponding expression for $\tilde{Y}_i$.

4.5.1 Remarks

The above surface is a simple bivariate B-spline product method which results in a C^2 freeform surface as well as provides shape control. This method is similar to a tensor product method but actually it is not. C^2 variable tensions are introduced in the B-splines which distinguish this surface method from the tensor product method and help in producing a C^2 surface which has tension control both locally and globally.

4.6 Interpolatory Surfaces

Expanding equation(4.20), we get the points through which the freeform rational B-spline surface passes, for given control points say P's. Here in our case we need to find P's (the new control points) given the data points F's, through which the interpolatory rational B-spline surface should pass. Let us denote it by F:

$$F_{i,j} = X = \tilde{\kappa}_i[P_{i-1,j-1}\kappa_j + P_{i-1,j}(\rho_j) + P_{i-1,j+1}\phi_j] + (\tilde{\rho}_j)[P_{i,j-1}\kappa_j + P_{i,j}(\rho_j) + P_{i,j+1}\phi_j] + \tilde{\phi}_i[P_{i+1,j-1}\kappa_j + P_{i+1,j}(\rho_j) + P_{i+1,j+1}\phi_j] \tag{4.22}$$

For $i = 1,\ldots,n$ and $j = 1,\ldots,m$; We can observe from the above that the sum of the coefficients of P's equal to unity, which means that the resulting interpolatory surface satisfies the *convex hull property*. Let

$$A_{i,j} = P_{i,j-1}\kappa_j + P_{i,j}\rho_j + P_{i,j+1}\phi_j \tag{4.23}$$

Equation(4.22) can be expressed as :

$$F = T.A \tag{4.24}$$

where F. T.and A are as given below:

$$T = \begin{bmatrix} \hat{\rho}_1 & \hat{\sigma}_1 & & & & \\ \hat{\kappa}_2 & \hat{\rho}_2 & \hat{\sigma}_2 & & & \\ & \hat{\kappa}_3 & \hat{\rho}_3 & \hat{\sigma}_3 & & \\ & & \hat{\kappa}_4 & \hat{\rho}_4 & \hat{\sigma}_4 & \\ & & & & & \\ & & & & & \\ & & & & \hat{\kappa}_m & \hat{\rho}_m \end{bmatrix}$$

$$A = \begin{bmatrix} A_{1,1} \\ A_{2,1} \\ . \\ . \\ \\ A_{m-1,1} \\ A_{m,1} \end{bmatrix} \quad \text{and} \quad F = \begin{bmatrix} F_{1,1} \\ F_{2,1} \\ \\ . \\ \\ F_{m-1,1} \\ F_{m,1} \end{bmatrix}$$

Since T is invertible. from equation(4.24). we get

$$A = T^{-1}.F \tag{4.25}$$

Moreover from equation(4.23). A can be expressed as:

$$A = D.P \tag{4.26}$$

The values of A, P, and D are as given below:

$$D = \begin{bmatrix} \rho_1 & \phi_1 & & & & \\ \kappa_2 & \rho_2 & \phi_2 & & & \\ & \kappa_3 & \rho_3 & \phi_3 & & \\ & & \kappa_4 & \rho_4 & \phi_4 & \\ & & & & & \\ & & & & \kappa_n & \rho_n \end{bmatrix}$$

$$A = \begin{bmatrix} A_{i,1} \\ A_{i,2} \\ . \\ . \\ A_{i,n-1} \\ A_{i,n} \end{bmatrix} \quad \text{and} \quad P = \begin{bmatrix} P_{i,1} \\ P_{i,2} \\ . \\ P_{i,n-1} \\ P_{i,n} \end{bmatrix}$$

So the new control points P's can be calculated as

$$P = D^{-1}.A \tag{4.27}$$

which when substituted in equation(4.20), gives the required interpolatory surface with interval and point tension which can be controlled both locally and globally.

4.6.1 Examples

The Figure 4.5 is a bicubic spline surface whereas the surface of Figure 4.6 is obtained because of high tension value 50 everywhere. The surface of Figure 4.7 demonstrate the result when tension is applied along a curve. Figure 4.8 and 4.9 show the effect of increase in point and interval tensions. Figure 4.10 shows the effect of increase in interval tension.

4.7 Concluding Remarks

We have described the basic theory for a C^2 rational cubic spline curve representation which has interval and point tension weights and which behaves in a well controlled and meaningful way. The extension to tensor product surface representations is immediately apparent. However, this representation exhibits a problem common to all tensor product descriptions in that the shape control parameters now effect a complete row or column of the tensor product array. [15] solves this problem for his cubic ν-spline representation by constructing a Boolean sum, spline-blended, rectangular-network of parametric ν-spline curves. We have followed the approach in [14] to overcome the above stated problem.

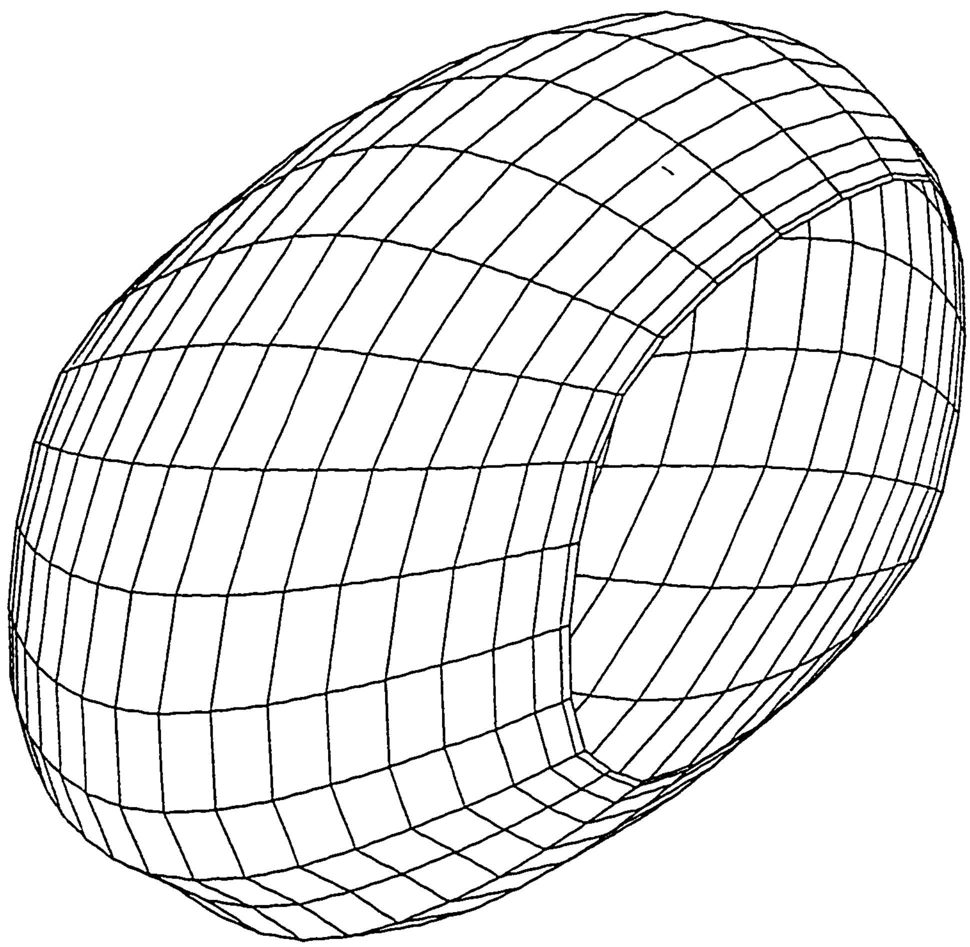

Figure 4.5: The bicubic spline surface

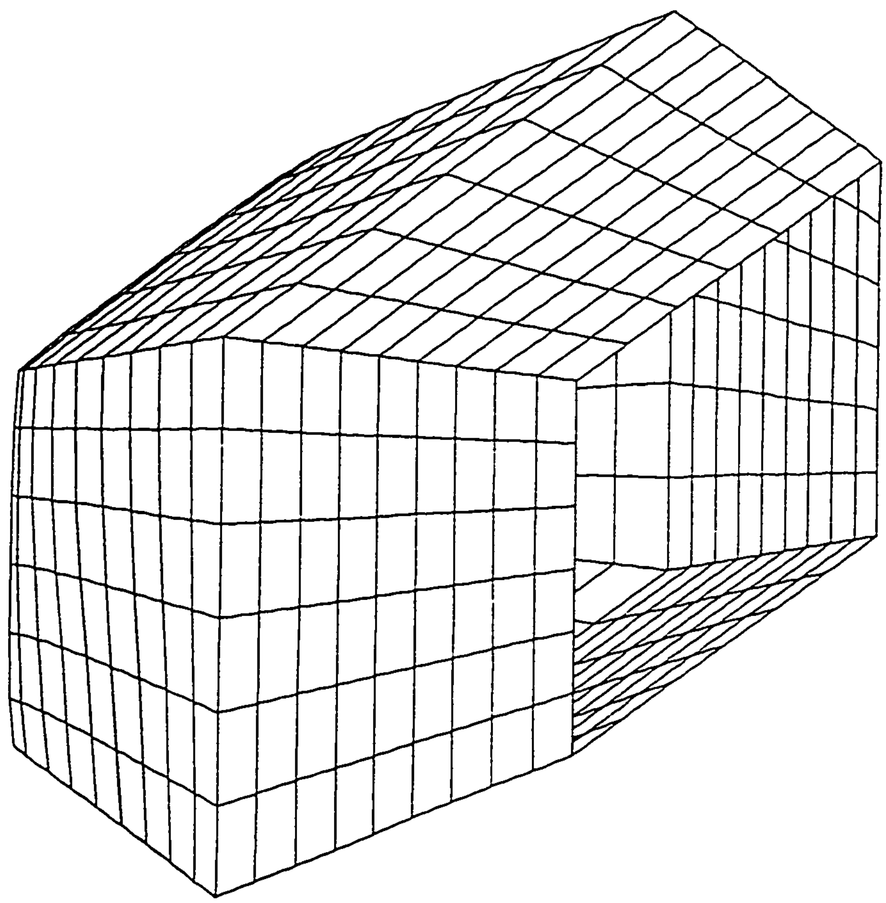

Figure 4.6: Global tension effect

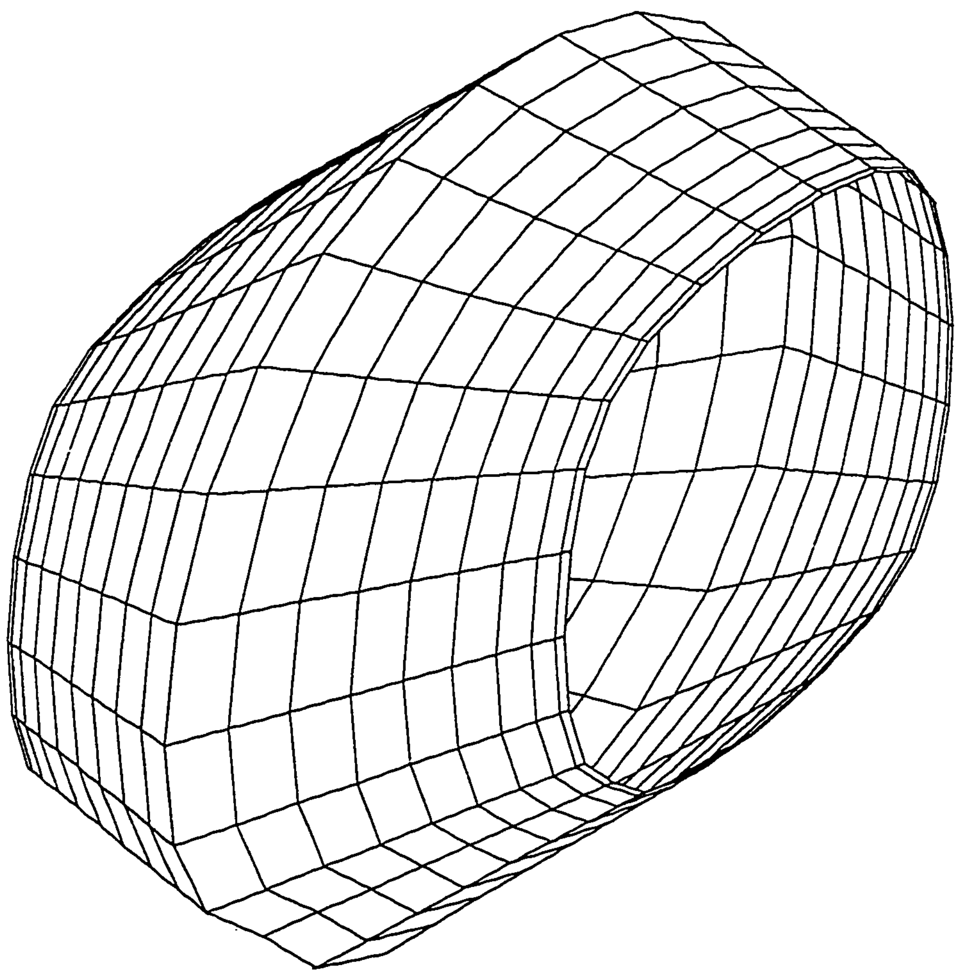

Figure 4.7: Tension along a curve

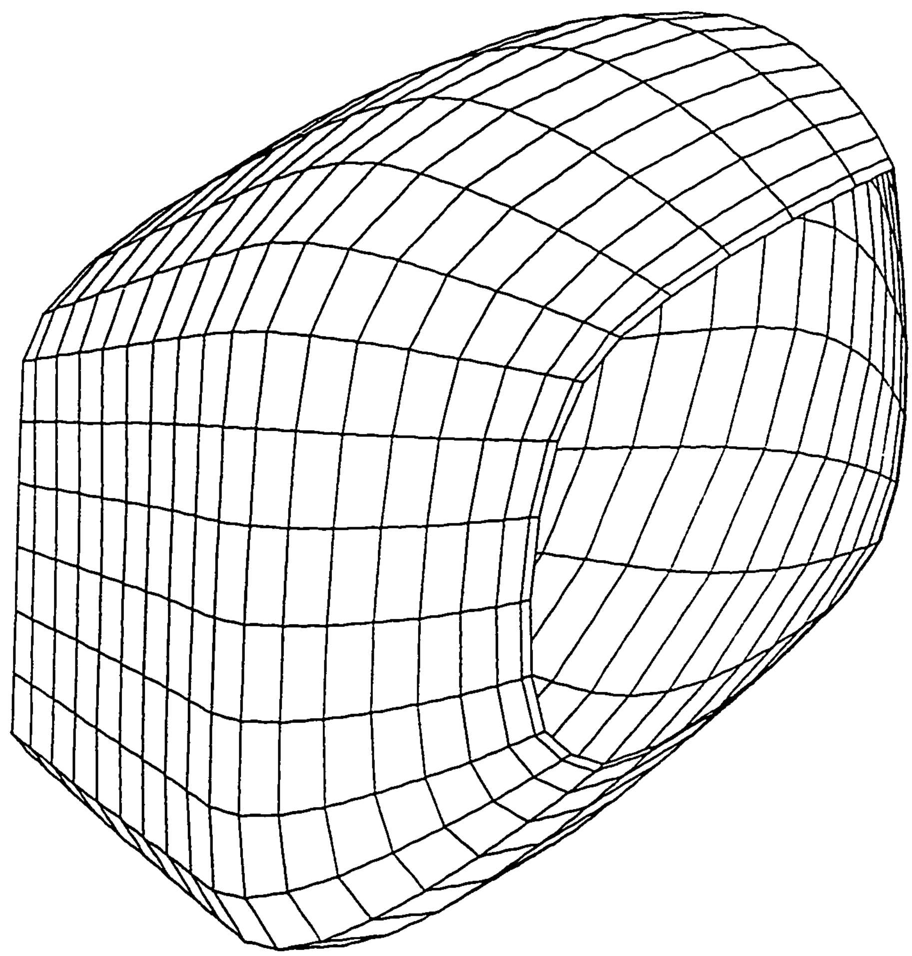

Figure 4.8: Point and interval tension effect

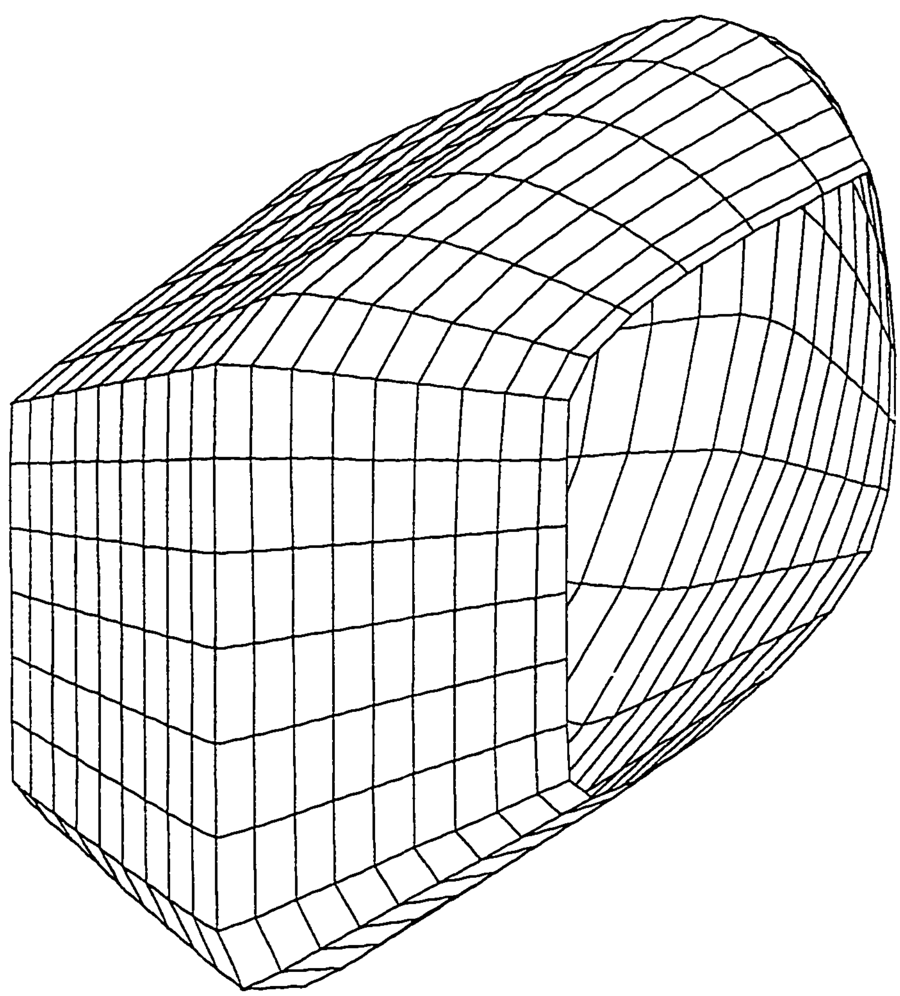

Figure 4.9: Point and interval tension effect

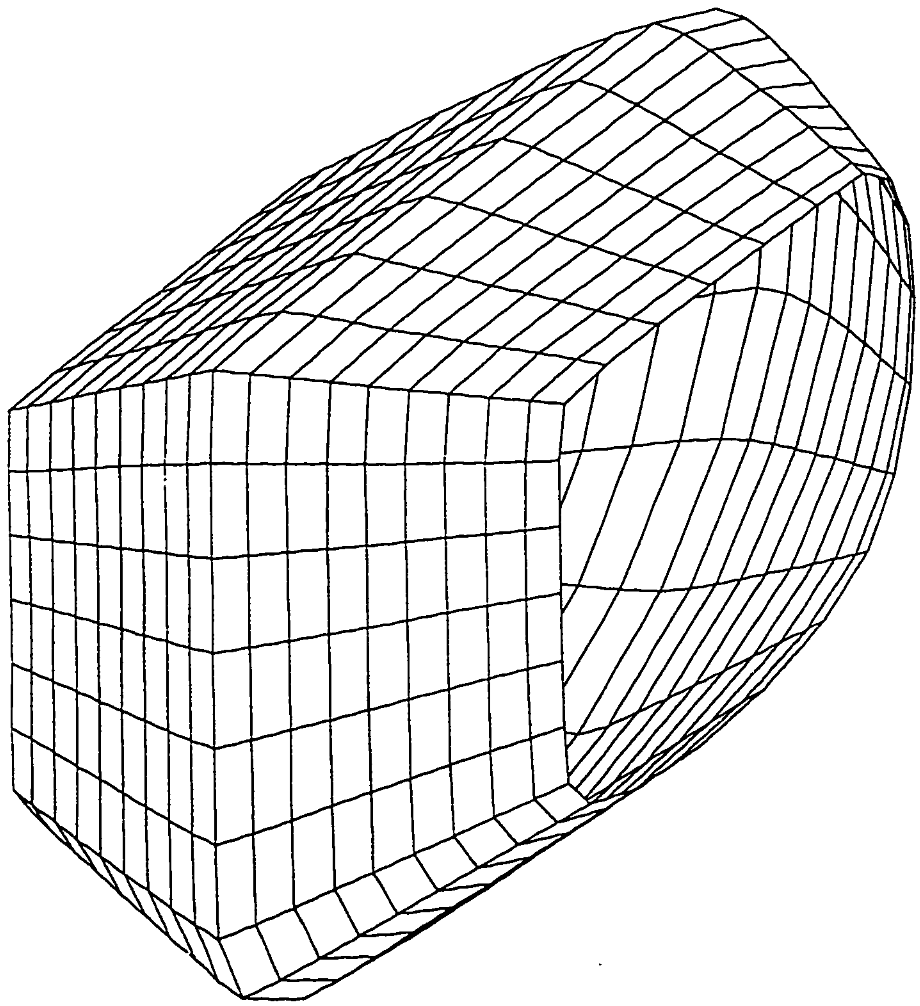

Figure 4.10: Interval tension effect

Chapter 5

CONCLUSIONS AND FUTURE WORK

5.1 Conclusions

5.1.1 C^2 Freeform Spline Curves and Corresponding Surfaces

A constructive way of developing the B-spline like basis functions of the C^2 rational cubic splines of [2] has been adopted. These basis functions and their corresponding design curve are reviewed with respect to two shape parameters in each interval. The method of computation is selected through the generation of the Bezier points from the control points, which makes the computations very convenient. Both local and global shape effects can be achieved in a well controlled way whereas NURBS do not have that much freedom.

The idea of the C^2 rational B-splines is quite simply generalized and extended to achieve a C^2 parametric rectangular freeform rational bicubic surface which can be controlled locally and globally. The surface has been designed through the sum of the products of bivariate rational B-spline basis functions. This is not a tensor product surface but a tensor product surface can be recovered as a special case. The tensor product surface is not that useful because any one of the tension parameters controls an entire corresponding interval strip of the surface. This is not a NURBS representation either; the NURBS representation of the surface has some limitations regarding its shape control. This surface is such that, one shape parameter is associated with each interval and one shape parameter is associated with each control point; these shape parameters can be used, both locally and globally, to tighten or loosen the surface along and/or across the network of curves associated with each knot. Computation of the surface has been suggested through the Bernstein-Bezier representation which is quite convenient.

5.1.2 C^2 Interpolatory Spline Curves and Corresponding Surfaces

The idea of C^2 freeform curves and surfaces have been extended to achieve corresponding C^2 interpolatory spline curves and surfaces, with a view to its application in CAGD. The interpolatory curves and surfaces satisfy all the properties of freeform curves and surfaces, namely local and global tension properties. In particular, it has been found that only one shape parameter per interval/knot is enough when local or global tension is required.

5.2 Future Work

1. Incorporation of geometric continuity, in addition to parametric continuity.

2. Incorporation of biased shape control parameter, apart from point and interval tension parameters.

3. Development of a recursive formula, like that of B-splines.

4. Use in visualization of data, as B-splines are being used for this purpose.

5. High quality character font designing.

Bibliography

[1] Thomas A. Foley. "Interpolation with Interval and Point Tension Controls Using Cubic Weighted ν-Splines ", *ACM Transaction on Mathematical Software*, vol. 13. no. 1, pp. 68–96, March 1987.

[2] Gregory J.A. and Sarfraz M.. "A Rational Cubic Spline with Tension", *Computer Aided Geometric Design*, vol. 7. pp. 1–13. 1990.

[3] Les Piegl, "On NURBS: A Survey", *IEEE Computer Graphics and Applications*. vol. 11, no. 1, pp. 55–71, January 1991.

[4] G.E Farin. *Curves and Surfaces for Computer Aided Geometric Design* . Academic Press. 1988.

[5] Boehm. W., Farin. G., and J. kahmann. "A Survey of Curve and Surface Methods in CAGD". *Computer Aided Geometric Design*, vol. 1. no. 1. pp. 1–360. 1984.

[6] Neilson. G. M.. *Some Piecewise Polynomial Alternatives to Splines under Tension. in R. E. Barnhill and R. F. Riesenfeld, eds.. Computer Aided Geometric Design*, Academic Press, New York, 1974.

[7] Preuss. S., "Properties of Splines in Tension", *J. Approx. Theory*, vol. 17, pp. 86–96, 1976.

[8] M.Sarfraz, "Spline Curve Interpolation with Shape Control", *M. Sc. Dissertation, Dept. of Mathematics and statistics. Brunel University, U.K.*, 1987.

[9] B.A Barsky, "Exponential and Polynomial Methods for Applying Tension to an Interpolating Spline Curves", *Comput. Vision Graph. and Image Process.*, vol. 27, pp. 1–18, 1984.

[10] Manning J. R, "Continuity Conditions for Spline Curves", *Comput. J*, vol. 17, no. 2, pp. 181–186, 1974.

[11] Nielson. G. M., "A Locally Controllable Spline with Tension for Interactive Curve Design", *Computer Aided Geometric Design*, pp. 199–205, 1984.

[12] Barsky. B. A., *The beta-spline: A local representation based on shape parameters and geometric measures* , PhD thesis. Dept. of Computer Science. The University of Utah, 1981.

[13] Boehm. W., "Curvature Continuous Curves and Surfaces", *Computer Aided Geometric Design*, vol. 2. no. 2, pp. 313–323. 1985.

[14] M.Sarfraz. "C^2 Rational B-Spline Surfaces with Tension Control". *New advances in CAD & Computer Graphics. International academic publishers. Beijing*, vol. 1. pp. 314–320. August 1993.

[15] Nielson. G. M., "Rectangular ν-splines". *IEEE Computer Graphics Applications*, vol. 6, pp. 35–40, 1986.

[16] Gordon. W. J., "Blending function methods of bivariate and multivariate interpolation and approximation", *SIAM J. Num. Anal.*, vol. 8, pp. 158–177, 1971.

[17] Muhammad Sarfraz, "Curves and Surfaces for Computer Aided Design using C^2 Rational Cubic Splines", *Engineering with Computers*, vol. 11, pp. 94–102, 1995.

[18] Muhammad Sarfraz, "A Rational B-Spline which does as an Alternative to the NURBs of Degree Three", Tech. Rep. TR/02/94. Dept. of Information and Computer Science, King Fahd University of Petroleum and Minerals, Dhahran - 31261, September 1994.

[19] M.Sarfraz, "A Rational Spline with Interval and Point Tension ", in *In Submission*, 1996.

Vita

- Mohammed Abdul Raheem
- Born in 1970. at Hyderabad, India.
- Received the Bachelor of Engineering degree in Computer Science and Engineering from Osmania University, Hyderabad in August, 1992.
- Joined the Information and Computer Sciences Department, King Fahd University of Petroleum and Minerals, Dhahran, Saudi Arabia, as a Research Assistant in September, 1993.
- Completed Masters Degree requirements in the Information and Computer Sciences Department in June 1996.